1955

Angular distribution of protons from Ca(44)(d.p.) CA(45) reaction

Cobb, Warrington C.; Guthe, Douglas B.

Massachusetts Institute of Technology

ANGULAR DISTRIBUTION OF PROTONS FROM $Ca^{44}(d,p)Ca^{45}$ REACTION

Warring Crane Cobb

and

Douglas Burden Guthe

PRP PROTONS
CAL CALCIUM

ANGULAR DISTRIBUTION OF PROTONS

FROM $Ca^{44}(d,p)Ca^{45}$ REACTION

a Cobb
val Academy

Guthe
val Academy

Letter on cover:

ANGULAR DISTRIBUTION OF PROTONS
FROM $Ca^{44}(d,p)Ca^{45}$ REACTION

Harrington Crane Cobb

and

Douglas Burden Guthe

llment of the

Degree of

ENCE

OF TECHNOLOGY

ANGULAR DISTRIBUTION OF PROTONS FROM $Ca^{44}(d,p)Ca^{45}$ REACTION

by

Warrington Crane Cobb
Lieutenant, U.S. Navy

and

Douglas Burden Guthe
Lieutenant, U.S. Navy

Submitted to the Department of Physics on May 23, 1955 in partial fulfillment of the requirements for the degree of Master of Science.

ABSTRACT

The MIT-ONR electrostatic generator and broad-range spectrograph have been used to study the angular distribution of proton groups from the reaction $Ca^{44}(d,p)Ca^{45}$. A thin target of $Ca^{44}O$, backed by Formvar and gold leaf, was bombarded with 7.0-Mev deuterons. The angular distributions for formation of the ground state and ten excited levels of Ca^{45} were observed.

The $Ca^{44}(d,p)Ca^{45}$ reaction was observed to proceed predominantly by stripping. The distributions have been compared with the predictions of the Butler stripping theory, in order to determine ℓ_n, the angular momentum of the captured neutron.

The angular momenta and parities for the levels of Ca^{45} have been determined as listed below:

Ca^{45} Level	ℓ_n	Possible Value of Spin	Parity
Ground State	3	5/2, 7/2	Odd
0.18 Mev	-	-	-
1.43 Mev	1	1/2, 3/2	Odd
1.89 Mev	1	1/2, 3/2	Odd
2.25 Mev	1	1/2, 3/2	Odd
2.40 Mev	0	1/2	Even
2.84 Mev	1 or 2	1/2, 3/2, 5/2	-
2.96 Mev	-	-	-
3.24 Mev	1 or 2	1/2, 3/2, 5/2	-
3.32 Mev	-	-	-
3.42 Mev	1 or 2	1/2, 3/2, 5/2	-

The relative differential cross sections for formation of the various levels have also been calculated.

The conclusions indicated that no single choice of the parameter r_o, the interaction radius of the Butler theory, resulted in unique determination of ℓ_n for all the distributions encountered. It has been suggested that the theory of Tobocman may give theoretical predictions to match the experimental results.

Thesis Supervisor: W. W. Buechner

Title: Associate Professor of Physics

The relative differential cross sections for formation of the various ions have also been calculated.

The conclusions indicated that no single studies of the cross-over ion, the interaction region of the Bethe theory, resulted in unique determination of ξ_0 for all the distributions encountered. It has been suggested that the theory of Thomson may give theoretical predictions to match the experimental results.

Thesis Supervisor: W. W. Buechner

Title: Associate Professor of Physics

A C K N O W L E D G M E N T S

The authors wish to express their appreciation to the entire staff of the High Voltage Laboratory for their friendly assistance and cooperation, without which this work could not have been accomplished.

In particular, we are very grateful to Professor Buechner for supervising this thesis, to Dr. C. K. Bockelman for his constant help and advice, and to Dr. C. P. Browne, Mr. A. Sperduto, Mr. S. Zimmerman, and Mr. R. Sharp for their patient consideration of our many questions.

We should also like to thank Mrs. Grace Rowe for her excellent job of drawing the curves and Misses Sylvia Darrow, Estelle Freedman, and Anna Recupero for their fine job of counting the photographic plates.

Finally, we wish to thank Mrs. Mary E. White for her excellent preparation of the manuscript.

ACKNOWLEDGMENTS

The authors wish to express their appreciation to the entire staff of the High Voltage Laboratory for their friendly assistance and cooperation, without which this work could not have been accomplished.

In particular, we are very grateful to Professor Thelmer for supervising this thesis, to Dr. G. E. Doolittle for his constant help and advice, and to Dr. C. F. Brown, Dr. A. Boyajian, Dr. S. Clampitt, and Mr. T. Clapp for their patient consideration of our many questions.

We should also like to thank Mrs. Grace Rees for her excellent job of drawing the curves and Misses Sylvia Lerner, Estella Trevelyan, and Anne Bellmore for their fine job of counting the photographic plates.

Finally, we wish to thank Mrs. Mary E. White for her excellent preparation of the manuscript.

TABLE OF CONTENTS

TABLES

TABLE OF CONTENTS

I. INTRODUCTION

The High Voltage Laboratory at the Massachusetts Institute of Technology has been investigating nuclear reactions involving calcium isotopes to provide experimental data upon which predictions of nuclear structure may be made. The calcium isotopes have closed shells of 20 protons. Ca^{40} has a closed shell of neutrons; the heavier calcium isotopes are formed by adding neutrons to the $1f_{7/2}$ shell until the shell is closed at Ca^{48}. Ca^{49} has one neutron in the $1f_{5/2}$ shell. Kurath[1] and Edmonds and Flowers[2] have made theoretical studies of the energy-level structure arising from configurations of two, three, and four identical particles in the $1f_{7/2}$ shell on the basis of the j-j coupling shell model. The latter authors point out that a transition from L-S to j-j coupling is anticipated in the region from A = 40 to 50. This Laboratory has made at least preliminary investigations of the energy levels of Ca^{40}[3], Ca^{41}[4], Ca^{42}, Ca^{43}[5], Ca^{44}, Ca^{45}[5], Ca^{48}, and Ca^{49}, and of the angular distributions of Ca^{41} and Ca^{43}[6].

This experiment investigates the angular distribution of protons from the reaction $Ca^{44}(d,p)Ca^{45}$. The Ca^{45} ground state has five neutrons in the $1f_{7/2}$ shell outside closed shells of 20 neutrons and 20 protons. Problems concerning the states that are formed by rearrangement of the five neutrons within the $1f_{7/2}$ shell may be treated the same analytically as the problem of 3 neutrons in the shell, according to the "hole" theory.

I. INTRODUCTION

The High Voltage Laboratory at the Massachusetts Institute of Technology has been investigating nuclear reactions involving calcium isotopes to provide experimental data upon which predictions of nuclear structure may be made. The calcium isotopes have closed shells of 20 protons. Ca_{20}^{40} has a closed shell of neutrons; the heavier calcium isotopes are formed by adding neutrons to the $1f_{7/2}$ shell until the shell is closed at Ca_{20}^{48}. Ca_{20}^{49} has one neutron in the $1f_{5/2}$ shell. Kurath[1] and Cohen and Flowers[2] have made theoretical studies of the energy-level structure arising from configurations of two, three, and four identical particles in the $1f_{7/2}$ shell on the basis of the 3-1 coupling shell model. The latter authors point out that a transition from L=3 to 3-1 coupling is anticipated in the region from A = 40 to 50. This laboratory has made at least preliminary investigations of the energy levels of Ca_{20}^{43}, Ca_{21}^{44}, Ca_{22}^{42}, Ca_{22}^{43}, Ca_{22}^{44}, Ca_{22}^{45}, Ca_{22}^{46}, and Ca_{20}^{49}, and of the angular distributions of Ca_{21}^{44} and Ca_{22}^{43}.

This experiment investigates the angular distribution of protons from the reaction $Ca_{22}^{44}(d,p)Ca_{22}^{45}$. The Ca_{22}^{45} ground state has five neutrons in the $1f_{7/2}$ shell outside closed shells of 20 neutrons and 20 protons. Problems concerning the states that are formed by rearrangement of the five neutrons within the $1f_{7/2}$ shell may be treated the same analytically as the problem of 3 neutrons in the shell, according to the "hole" theory.

The angular distributions of protons from (d,p) reactions are often characterized by pronounced maxima in the forward direction. In order to explain these reactions without postulating high values of angular momentum, the stripping process has been visualized. The Butler[7] theory predicts the angular distributions of protons from these (d,p) reactions in terms of "ℓ_n", the angular momentum of the captured neutron. Butler's calculations indicate that for $\ell_n = 0$, the maximum of the angular distribution occurs near $\theta = 0$, where θ is the angle of observation. As the characteristic value of ℓ_n is increased, the maximum of the angular distribution moves to larger values of θ. If the angular momentum and parity of the initial nucleus in the reaction are known, determination of ℓ_n corresponding to the formation of a given level in the final nucleus also determines the parity and possible values of angular momentum for that level. Greater restrictions may be placed on the possible values of angular momentum for the level if I = 0 for the initial nucleus.

In this experiment, the Butler theory has been used to investigate the parities and angular momenta of the ground state and ten excited levels of Ca^{45}[8], listed in Table I.

Ca^{45} decays by beta emission to Sc^{45}. The measured values for Sc^{45} of I = 7/2[9] and μ = 4.76[10]* point to a $f_{7/2}$ ground state because of the position of Sc^{45} on the Schmidt diagram. This is as predicted by the extreme single-particle shell model. The β^- decay has a half-life of 163.5 days[11] and an allowed shape on the Kurie plot with E_{max} =

*nuclear magnetons.

The angular distribution of protons from (d,p) reactions are often characterized by pronounced maxima in the forward direction. In order to explain these reactions without postulating high values of angular momentum, the stripping process has been advanced. The Butler[7] theory predicts the angular distributions of protons from (d,p) reactions in terms of "l_n", the angular momentum of the captured neutron. Butler's calculations indicate that for $l_n = 0$, the maximum of the angular distribution occurs near $\vartheta = 0°$, where ϑ is the angle of observation. As the characteristic value of l_n is increased, the maximum of the angular distribution moves to larger values of ϑ. If the angular momentum and parity of the initial nucleus in the reaction are known, determination of l_n corresponding to the formation of a given level in the final nucleus also determines the parity and possible values of angular momentum for that level. Certain restrictions may be placed on the possible values of angular momentum for the level if $I = 0$ for the initial nucleus.

In this experiment, the Butler theory has been used to investigate the parities and angular momenta of the ground state and ten excited levels of Cu^{65}, listed in Table I.

Cu^{65} decays by beta emission to Zn^{65}. The measured values for Cu^{65} of $I = 3/2$, and $\mu = 1.75$ nm* point to a $f_{3/2}$ ground state because of the position of Na^{23} on the Mosely diagram. This is as predicted by the extreme single-particle shell model. The β^- decay has a half-life of 13.5 days[11] and an allowed shape on the Kurie plot with $E_{max} =$

*nuclear magnetons.

TABLE I

Excited Levels of Ca^{45}

0	Ground state
1	0.18 Mev
2	1.43 Mev
3	1.89 Mev
4	2.25 Mev
5	2.40 Mev
6	2.84 Mev
7	2.96 Mev
8	3.24 Mev
9	3.32 Mev
10	3.42 Mev

0.255 Mev[12]. This leads to log ft = 5.9. If then the β^- transition is taken to be an allowed one, the result is not in disagreement with the extreme single-particle shell-model prediction of $f_{7/2}$ for the ground state of Ca^{45}. Since I = 0 for the ground state of Ca^{44}, the angular distribution of the protons associated with the formation of the ground state of Ca^{45} is expected to be characterized by $\ell_n = 3$.

The MIT-ONR electrostatic generator and broad-range magnetic spectrograph have been used to study the angular distributions of proton groups resulting from deuteron bombardment of a thin $Ca^{44}O$

TABLE I

Excited levels of Ca^{45}

0	Ground state
1	0.13 Mev
2	1.63 Mev
3	1.89 Mev
4	2.55 Mev
5	2.40 Mev
6	2.81 Mev
7	2.96 Mev
8	3.24 Mev
9	3.32 Mev
10	3.42 Mev

0.255 Mev[12]. This leads to $J_{\pi} = 5^{+}$. If then the β^{-} transition is taken to be an allowed one, the result is not in disagreement with the extreme single-particle shell-model prediction of $f_{7/2}$ for the ground state of Ca^{45}. Since I = 0 for the ground state of Ca^{44}, the angular distribution of the neutrons associated with the formation of the ground state of Ca^{45} is governed by $\ell_n = 3$.

The MIT-ONR electrostatic generator and time-of-flight apparatus have been used to study the angular distributions of proton groups resulting from deuteron bombardment of a thin $Ca^{44}O$ -

target. The investigation has been carried out at an energy of 7.0 Mev. The proton groups associated with the ground state and the ten excited levels of Ca^{45} have been observed at eighteen angles between 7-1/2 and 120 degrees.

II. EXPERIMENTAL PROCEDURE AND APPARATUS

Charged particles emerging from the bombarded target were deflected in the magnetic field of the spectrograph and then detected on Eastman NTA 25μ photographic plates. The positions of the tracks along the plates determine the radii of curvature of the particles. Calibration of the various distances along the plates was made previously by comparison with the position of alpha-particles from polonium deflected by a known spectrographic field. This procedure has been described elsewhere[16]. The plates were read by counting the number of tracks within each half-millimeter section along the plates. The total length of photographic plate exposed in one run is approximately 76 centimeters. To facilitate plate reading, the plates were covered with thin layers of aluminum foil during exposure on (d,p) runs to prevent charged particles heavier than protons from reaching the emulsion. Detailed descriptions of the MIT-ONR electrostatic generator and the broad-range spectrograph have been given elsewhere[13-15].

The target used was prepared by C. M. Braams, presently at the University of Utrecht, while working at this Laboratory. The method was evaporation of CaO onto a thin film of Formvar, backed by gold leaf. The enriched Ca^{44} isotope was received in the form of $CaCO_3$ from the U. S. Atomic Energy Commission, Stable Isotopes Division, Oak Ridge, Tennessee. The calcium content was 97.99 percent Ca^{44}; the impurity was mainly Ca^{40}.

II. EXPERIMENTAL TECHNIQUES AND CONCEPTS

Charged particles emerging from the bombarded target were deflected in the magnetic field of the spectrograph and then recorded on Eastman NTA 25μ photographic plates. The positions of the tracks along the plates determine the radii of curvatures of the particles. Calibration of the various distances along the plates was made previously by comparison with the position of alpha-particles from polonium deflected by a known spectrographic field. This procedure has been described elsewhere[16]. The plates were read by counting the number of tracks within each half-millimeter position along the plates. The total length of photographic plate exposed in one run is approximately 75 centimeters. To facilitate plate reading, the plates were covered with thin layers of aluminum foil during exposure on (d,p) runs to prevent charged particles heavier than protons from reaching the emulsion. Detailed descriptions of the NTA-type photographic processing and the broad-range spectrograph have been given elsewhere[13-15].

The target used was prepared by G. H. Jenkins, presently at the University of Utrecht, while working at this laboratory. The method was evaporation of CaO onto a thin film of Formvar, backed by gold leaf. The evaluated Ca^{48} isotope was received in the form of $CaCO_3$ from the U. S. Atomic Energy Commission, stable Isotopes Division, Oak Ridge, Tennessee. The calcium content was 97.99 percent Ca^{48}, the impurity was mainly Ca^{40}.

The Butler curves shown in the results were constructed from nomograms prepared by C. R. Lubitz and W. C. Parkinson of the University of Michigan[17].

III. EXPERIMENTAL RESULTS

In order to determine the strong contaminants in the target, a survey was made by bombarding the target with 6-Mev protons and analyzing the elastically scattered proton groups for the masses of the scattering nuclei. The results of this survey are presented in Figure 1. A 400-microcoulomb exposure was used with a spectrograph angle of 120 degrees. The peak for gold is approximately 250-kev wide at the bottom, thereby obscuring any contaminants of masses between 50 and 197.

A preliminary bombardment of the target with 7-Mev deuterons was made, using an exposure of 500 microcoulombs, and a spectrograph angle of 30 degrees. The resulting proton groups were studied to verify the presence of energy levels of Ca^{45}, as found by C. M. Braams. An additional verification was later provided by noting that the energy of proton groups attributed to Ca^{45} had the correct dependence upon θ.

The preliminary bombardment provided information on the intensities of the various Ca^{45} levels. This information was used to determine the exposures required to observe the levels with good statistics.

Experimental data for the angular distribution of Ca^{45} were obtained with two bombardment exposures at each angle up to 60 degrees, because of the differences in the intensities of the proton groups

XII. EXPERIMENTAL RESULTS

To verify to determine the atomic configuration in the target, a survey was made by bombarding the target with 6-Mev protons and analyzing the elastically scattered protons given for the beams of the scattering nuclei. The results of this survey are presented in Figure 7. A 100-microcoulomb exposure was used with a scattering angle of 110 degrees. The peak for gold is approximately 250-fold as at the bottom, thereby observing any contaminants of masses between 50 and 197.

A preliminary bombardment of the target with 7-Mev deuterons was made, using an exposure of 500 microcoulombs, and a scattering angle of 30 degrees. The resulting proton groups were studied to verify the presence of energy levels of Ca^{42}, as found by O. Ha. Lassen. An additional verification was later provided by making that the energy of proton groups attributed to Ca^{42} had the correct dependence upon θ.

The preliminary bombardment provided information on the intensities of the various Ca^{42} levels. This information was used to determine the exposures required to observe the levels with good statistics.

Experimental data for the angular distribution of Ca^{42} were obtained with the bombardment extending at each angle to 60 degrees, because of the differences in the intensities of the proton groups

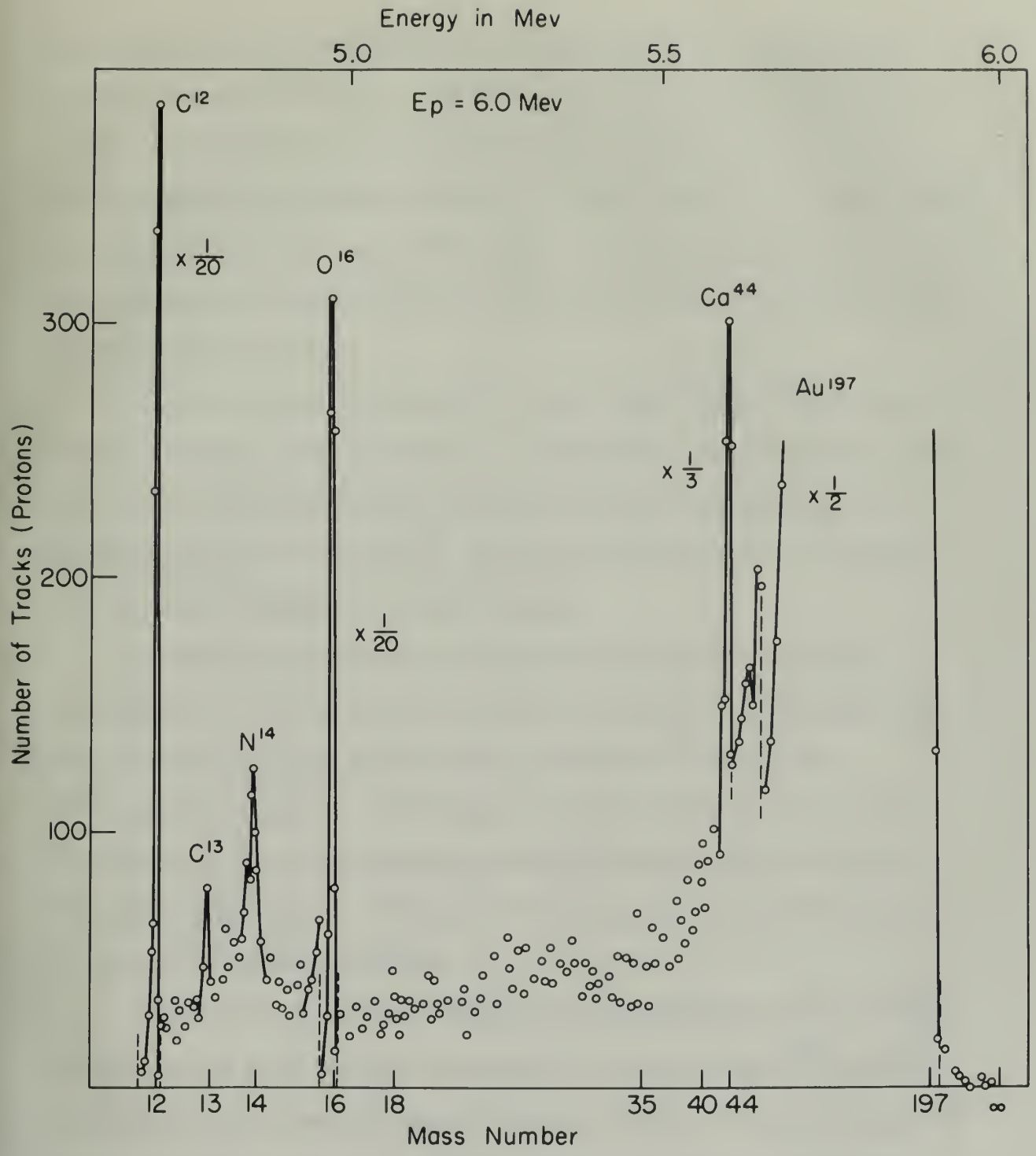
Energy in Mev
5.0
5.5
6.0
Ep = 6.0 Mev
C12
x 1/20
O16
Ca44
Au197
x 1/3
x 1/2
x 1/20
N14
C13
300
200
100
Number of Tracks (Protons)
12
13
14
16
18
35
40
44
197
∞
Mass Number

Figure 1

associated with the formation of the various levels. A 3000-microcoulomb exposure was used to obtain data for the groups corresponding to the ground state and to the 0.18, 2.40, 2.96, and 3.32 Mev levels; a 500-microcoulomb exposure was used to obtain data for the groups corresponding to the 1.43, 1.89, 2.25, 2.84, 3.24, and 3.42 Mev levels. All data obtained at angles from 70 to 120 degrees were obtained with a 500-microcoulomb exposure.

Figure 2 shows representative data obtained with a 500-microcoulomb exposure. The half-widths of the peaks observed in the experiment varied generally from 1.8 to 3.0 millimeters, corresponding to energy spreads of 16 to 23 kev. The peak width was due to a combination of target thickness and slit opening.

Because of the presence of carbon and oxygen in the target, some levels of Ca^{45} could not be observed at certain angles since they were masked by intense proton groups from the $C^{12}(d,p)C^{13}$ and $O^{16}(d,p)O^{17}$ reactions. This situation is made clear in Figure 2 by the intensity of the proton group corresponding to the formation of the ground state of C^{13}. Table II tabulates the data missing because of carbon and oxygen reactions.

All levels of Ca^{45} were obscured at the 5-degree angle of observation because of an intense background of protons from $Al^{27}(d,p)Al^{28}$ reactions in the aluminum foil covering the plates. At small angles of observation, the number of deuterons scattered into the spectrograph becomes very high.

associated with the formation of the various levels. A 3000-micro-coulomb exposure was used to obtain data for the groups corresponding to the ground state and to the 0.18, 2.10, 2.96, and 3.32 Mev levels; a 500-microcoulomb exposure was used to obtain data for the groups corresponding to the 1.43, 1.69, 2.25, 2.83, 3.23, and 3.42 Mev levels. All data obtained at angles from 70 to 120 degrees were obtained with a 500-microcoulomb exposure.

Figure 2 shows representative data obtained with a 500-microcoulomb exposure.- The half-widths of the peaks observed in the experiment varied generally from 1.8 to 3.0 millimeters, corresponding to energy spreads of 16 to 23 kev. The peak width was due to a combination of target thickness and slit opening.

Because of the presence of carbon and oxygen in the target, some levels of Ca^{42} could not be observed at certain angles since they were masked by intense proton groups from the $C_{12}(d,p)C_{13}$ and $O_{16}(d,p)O_{17}$ reactions. This situation is made clear in Figure 2 by the intensity of the proton group corresponding to the formation of the ground state of C_{13}. Table II tabulates the data showing presence of carbon and oxygen reactions.

All levels of Ca^{42} were observed at the 5-degree angle of observation because of an intense background of protons from $Al_{27}(d,p)Al_{28}$ reactions in the aluminum foil covering the plates. At small angles of observation, the number of deuterons scattered into the spectrograph become very high.

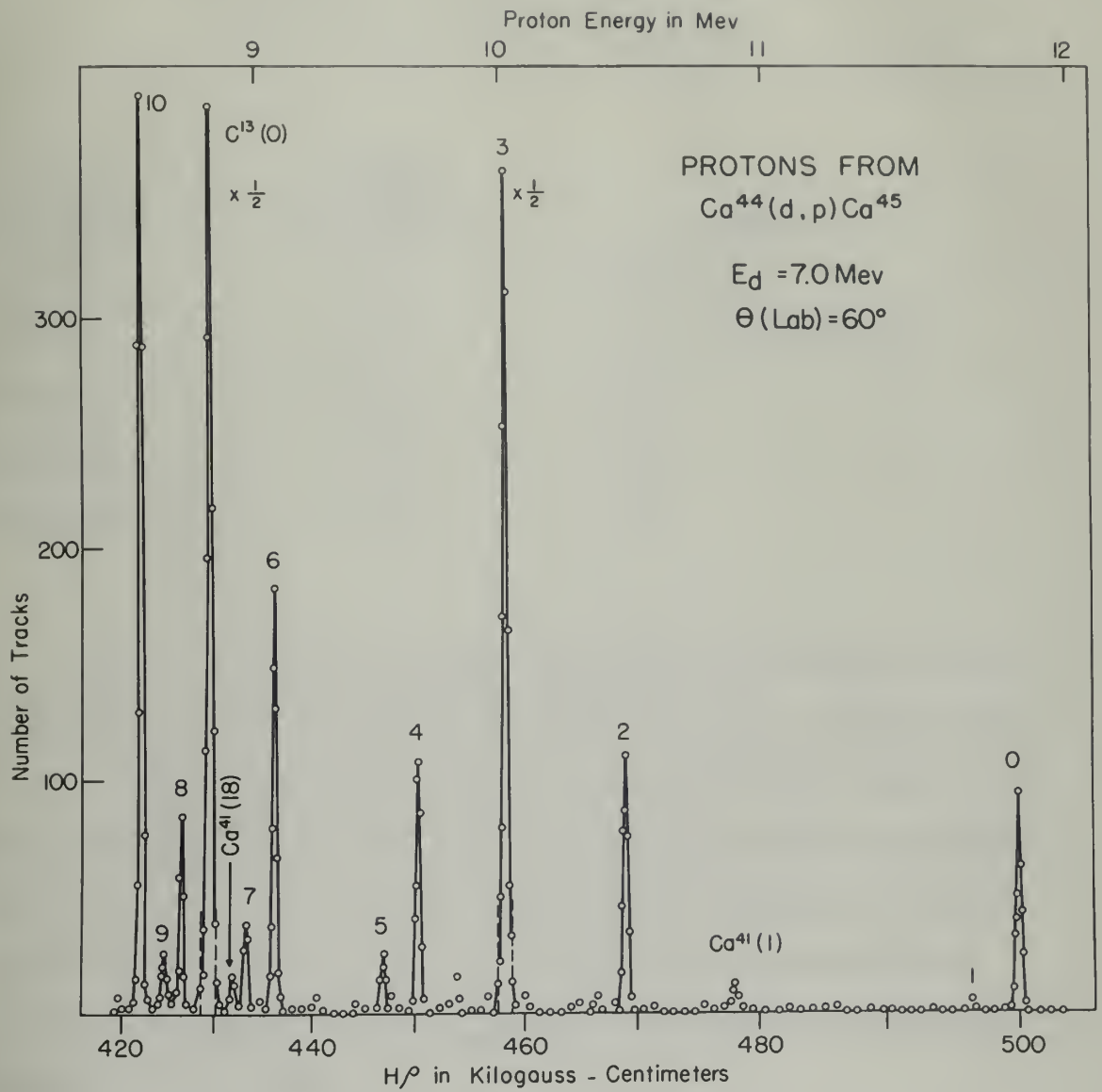
Proton Energy in Mev
9
10
11
12
PROTONS FROM
Ca44(d,p)Ca45
Ed = 7.0 Mev
θ (Lab) = 60°
C13 (0)
x 1/2
x 1/2
Ca41 (18)
Ca41 (1)
10
9
8
7
6
5
4
3
2
1
0
300
200
100
Number of Tracks
420
440
460
480
500
Hρ in Kilogauss - Centimeters

Figure 2

TABLE II

Data Missing Because of Interference from
$C^{12}(d,p)C^{13}$ and $O^{16}(d,p)O^{17}$ Reactions

Obscured Ca^{45} Level	Reaction Product Responsible	Angle
3.42 Mev	$O^{17}(0)$	30°, 35°
3.32 Mev	$O^{17}(0)$	7-1/2°, 10°, 15°, 20°
3.32 Mev	$C^{13}(0)$	70°
2.96 Mev	$C^{13}(0)$	50°
2.84 Mev	$C^{13}(0)$	45°

While observing the angular distribution of protons, the magnetic field of the spectrograph was varied from run to run to cause the ground-state proton group to be observed at the same place on the photographic plates at each angle of observation; this in fact caused the other Ca^{45} proton groups to remain almost stationary. This procedure obviated the need for a solid-angle correction caused by a given proton group appearing at different positions as the angle of observation was varied.

To insure that there was no change in the target which might have affected the intensities of the observed proton groups during the successive runs at the various angles, normalizing runs were periodically made at an angle of 60 degrees. The sum of the number of tracks

TABLE II

Data Bearing Upon the Interference Between
$O_{12}(4^+,5)2_{13}$ and $O_{16}(4^+,5)O_{17}$ Resonances

Observed O_{16} Level	Interaction Product Responsible	Angle
3.12 Mev	$O_{17}(0)$	30^o, 35^o
3.32 Mev	$O_{17}(0)$	$7-1/2^o$, 10^o, 15^o, 20^o
3.38 Mev	$O_{13}(0)$	70^o
2.96 Mev	$O_{13}(0)$	50^o
2.64 Mev	$O_{13}(0)$	45^o

data observing the angular distribution of protons, the magnetic field of the spectrograph was varied from run to run to cause the ground-state proton group to be observed at the same place on the photographic plates at each angle of observation; this in turn caused the other O_{16} proton groups to remain almost stationary. This circumstance obviated the need for a solid-angle correction caused by a given proton group appearing at different positions as the angle of observation was varied.

It leaves that there was no change in the isotopic which might have affected the intensities of the observed proton groups during the successive runs at the various angles, necessitating runs were periodically made at an angle of 60 degrees. The use of the number of times

corresponding to the ground state and to the 1.43- and 2.25-Mev levels was counted for comparison. Normalizing runs were made with an exposure of 500 microcoulombs. Table III outlines the method and results of the normalizing procedure. The results indicate that there was no change in the target.

It was also necessary to insure that a change in the angle of observation, θ, did not change the solid angle subtended by the defining slits which are just in front of the photographic plate. To accomplish this, the target was rotated 90 degrees, from -45 degrees from the beam axis to +45 degrees, between runs 5 and 6. As can be seen from the diagram below

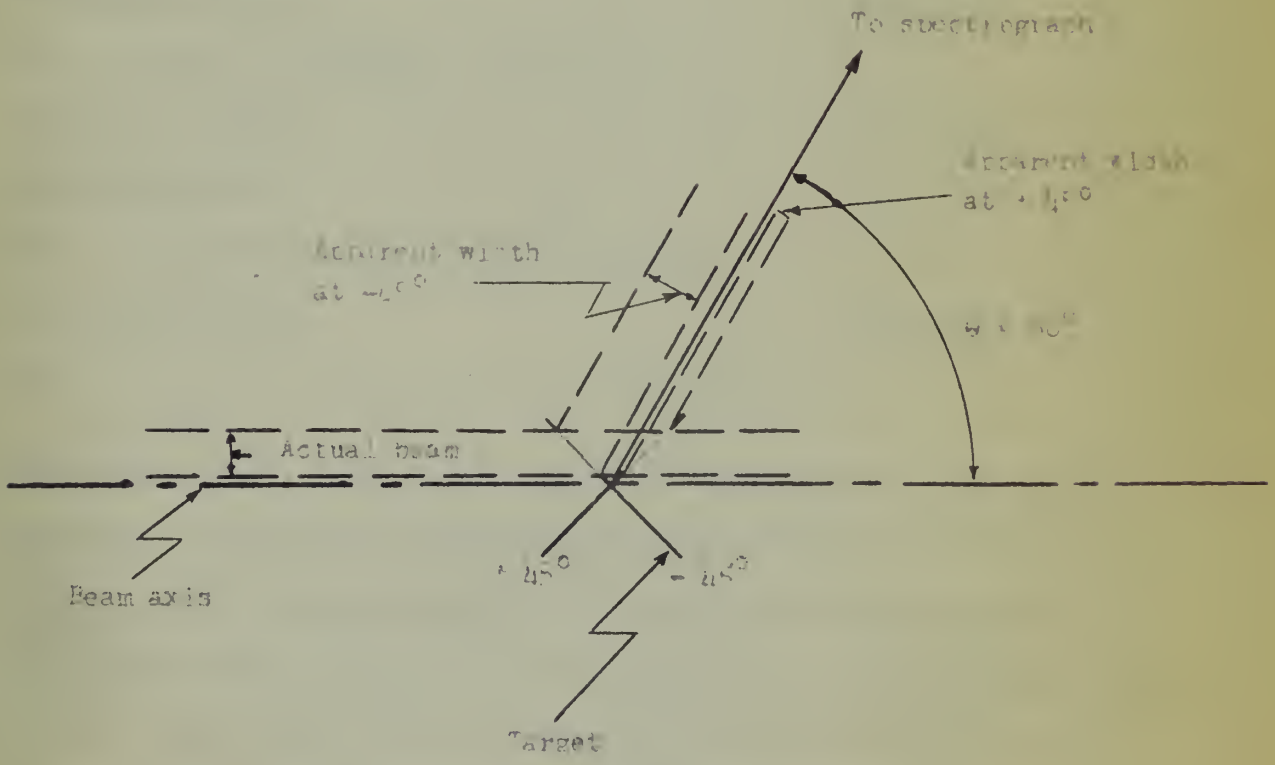

TABLE III

Normalizing Procedure

Order of Runs	Total counts in ground state and 1.43- and 2.25-Mev proton groups ± standard deviation
Normalizing run 1	1393 ± 37
Runs at 50, 40, 30, 20, 10 degrees	
Normalizing run 2	1320 ± 36
Runs at 60, 55, 45, 35, 25, 15 degrees	
Normalizing run 3	1489 ± 39
Normalizing run 4	1443 ± 38
Runs at 7-1/2, 5 degrees	
Normalizing run 5	1472 ± 38
Normalizing run 6	1437 ± 38
Runs at 70, 90, 110, 120, 100, 80 degrees	
Normalizing run 7	1416 ± 38

this rotation did not change the area of the target which was illuminated by the beam even if the beam had been off center; however, it did change the apparent width of the beam spot as viewed from the spectrograph. Since the intensity of the peaks did not change between runs 5 and 6, this indicates that the apparent width of the beam spot did not affect the solid angle observed by the spectrograph.

TABLE III

Normalizing Procedure

Order of Runs	Total counts in proton peaks and 1.63- and 1.65-Mev proton groups ± standard deviation
Normalizing run 1	1393 ± 37
Runs at 50°, 40°, 30°, 20°, 10 degrees	
Normalizing run 2	1320 ± 36
Runs at 60°, 55°, 45°, 35°, 25°, 15 degrees	
Normalizing run 3	1409 ± 38
Normalizing run 4	1443 ± 38
Runs at 7-1/2°, 5 degrees	
Normalizing run 5	1472 ± 38
Normalizing run 6	1437 ± 38
Runs at 70°, 90°, 110°, 120°, 100°, 80 degrees	
Normalizing run 7	1416 ± 38

this rotation did not change the area of the target which was illuminated by the beam even if the beam had been off center; however, it did change the apparent width of the beam spot as viewed from the spectrograph. Since the intensity of the peaks did not change between runs 5 and 6, this indicates that the apparent width of the beam spot did not affect the solid angle observed by the spectrograph.

Figures 3 through 21 show the experimental angular distributions plotted with the calculated Butler curves. The errors shown represent the statistical counting errors only, based on a standard deviation. The spectrograph accepted particles with angles 1/4 degree either side of the nominal angle Θ.

The Butler curves, as plotted, are not corrected for the difference between Θ_{lab} and $\Theta_{C.M.}$ or for the difference between the solid angle in laboratory and solid angle in center-of-mass coordinates.

Using the formulas,

$$\tan \Theta_{lab} = \frac{\sin \Theta_{C.M.}}{\gamma + \cos \Theta_{C.M.}}$$

$$\gamma = \sqrt{\frac{m_1 m_3}{m_2 m_4} \frac{E_d \text{ in C. M.}}{E_d \text{ in C.M.} + Q}}$$

$m_1 \triangleq M_{deuteron}$

$m_2 \triangleq M_{Ca44}$

$m_3 \triangleq M_{proton}$

$m_4 \triangleq M_{Ca45}$

$$E_d \text{ in C.M.} = \frac{m_2}{m_1 + m_2} E_{d_{lab}}$$

and $$\frac{d\Omega_{C.M.}}{d\Omega_{lab}} = \cos (\Theta_{C.M.} - \Theta_{lab}) \left(\frac{\sin \Theta_{lab}}{\sin \Theta_{C.M.}}\right)^2 ,$$

one gets the following results for the tenth excited level at 3.42 Mev:

$\Theta_{C.M.}$	Θ_{lab}	$\Delta\Theta$	$\frac{d\Omega_{C.M.}}{d\Omega_{lab}}$
10°	$9^\circ 43'$	$17'$	0.944
50°	$48^\circ 48'$	$1^\circ 12'$	0.967

Figures 3 through 21 show the experimental angular distributions plotted with the calculated Butler curves. The corresponding theoretical curves, based on a standard deviation of the nominal angle θ.

The Butler curves, as plotted, are not convoluted for the difference between θ_{lab} and $\theta_{c.m.}$ or for the difference between the solid angle in laboratory and solid angle in center-of-mass coordinates. Using the formulas,

$$\tan\theta_{lab} = \frac{\sin\theta_{c.m.}}{\gamma + \cos\theta_{c.m.}} \qquad m_2 \triangleq \text{mass of } b$$

$$\gamma = \sqrt{\frac{m_1 m_3}{m_2 m_4}\frac{E_d}{E_d}\frac{\text{kinematic factor}}{\text{kinematic factor}} + Q} \qquad m_3 \triangleq \text{mass of } c$$

$$m_4 \triangleq \text{mass of } d$$

$$E_d \text{ in c.m.} = \frac{m_3}{m_1 + m_2} E_{d\,lab}$$

and $$\frac{d\sigma_{lab}}{d\sigma_{c.m.}} = \cos(\theta_{c.m.} - \theta_{lab})\left(\frac{\sin\theta_{lab}}{\sin\theta_{c.m.}}\right)^2 ,$$

the ends the following results for the tenth excited level at 3.42 Mev:

$\theta_{c.m.}$	θ_{lab}	θ	$\frac{d\sigma_{c.m.}}{d\sigma_{lab}}$
5°	$4^\circ 43'$	5°	0.947
10°	$9^\circ 23'$	10°	0.894

The corrections for this state are largest, since it has the lowest Q-value. Over the range of interest, $\theta = 10^{\circ}$ to 50°, where the maxima occur, both corrections are smaller than the error introduced by the nomogram.

One undetermined parameter in the calculation of the angular distribution in the Butler theory is the interaction radius, r_o. Huby[18] has stated that Gamov's[19] formula

$$r_o = (1.22\ A^{1/3} + 1.7) \times 10^{-13} \text{ cm.}$$

gives a radius which will normally support unique determinations of ℓ_n. This formula gives $r_o = 6.0 \times 10^{-13}$ cm. for Ca^{45}. The results of this experiment indicate that no one value for r_o will lead to unique values of ℓ_n; therefore, the experimental data have been presented with Butler curves employing $r_o = 6.0$ and 7.0 on Figures 3 through 21.

The experimental data on Figures 3 through 21 have been interpreted as follows:

Figures 3 and 4 illustrate the ground-state distribution. It is characterized by $\ell_n = 3$; $r_o = 7.0$ provides the best fit.

The 0.18-Mev level is not illustrated. The state was detected at the indicated energy but was observed with such low intensity that the angular distribution could not be determined.

Figures 5 and 6 illustrate the 1.43-Mev level distribution. It is characterized by $\ell_n = 1$; $r_o = 6.0$ provides the best fit.

The correction for this style was simple, since it has the least χ^2-value. Over the range of interest, $\theta = 12^0$ to 50^0, where the results occur, both corrections are smaller than the error introduced by the measures.

One theoretical parameter is the calculating of the angular distribution in the Butler theory is the interaction radius, r_0. Ruby[12] has quoted that formula r_0 formula

$$r_0 = (1.22 A^{1/3} + 1.7) \times 10^{-13} \text{ cm}.$$

gives a radius which will normally account within observations of ℓ_n. This formula gives $r_0 = 6.0 \times 10^{-13}$ cm. for Cu^{65}. The results of this experiment indicate that no one value for r_0 will lend to unique values of ℓ_n; therefore, the experimental data have been presented with Butler curves employing $r_0 = 6.0$ and 7.0 on Figures 3 through 21.

The experimental data on Figures 3 through 21 have been interpreted as follows:

Figures 3 and 4 illustrate the ground-state distribution. It is characterized by $\ell_n = 3$; $r_0 = 7.0$ provides the best fit.

The 0.12-Mev level is not illustrated. The graphs was observed as the indicated energy bin was observed with such low intensity that the angular distribution could not be determined.

Figures 5 and 6 illustrate the 1.23-Mev level distribution. It is characterized by $\ell_n = 1$; $r_0 = 6.0$ provides the best fit.

Figures 7 and 8 illustrate the 1.89-Mev level distribution. It is probably an $\ell_n = 1$ distribution; $r_o = 6.0$ provides the best fit.

Figures 9 and 10 illustrate the 2.25-Mev level distribution. It is characterized by $\ell_n = 1$; $r_o = 6.0$ provides the best fit.

Figures 11 and 12 illustrate the 2.40-Mev level distribution. It is characterized by $\ell_n = 0$.

Figures 13 and 14 illustrate the 2.84-Mev level distribution. It is probably an $\ell_n = 2$ distribution; however, the fit is somewhat ambiguous at both values of r_o.

Figure 15 illustrates the 2.96-Mev level distribution. No determination of ℓ_n is possible. The asymmetry about 90 degrees suggests that stripping action takes place in the formation of this level, but it does not appear to be the characteristic "Butler" type.

Figures 16 and 17 illustrate the 3.24-Mev level distribution. It is probably an $\ell_n = 2$ distribution; the fit is ambiguous with $r_o = 6.0$.

Figures 18 and 19 illustrate the 3.32-Mev level distribution. The data do not justify the assignment of ℓ_n. There is doubt whether the characteristic "Butler" type stripping takes place in the formation of this level. For comparison only, $\ell_n = 3$ curves are shown.

Figures 20 and 21 illustrate the 3.42-Mev level distribution. It is probably an $\ell_n = 2$ distribution, but the fit is poor. The assignment of ℓ_n might have been more definite had the level not been obscured at 30 and 35 degrees.

Figures 7 and 8 illustrate the 1.8σ-km level distribution. It is probably an ℓ^n = 1 distribution; r_o = 6.0 provides the best fit.

Figures 9 and 10 illustrate the 2.2σ-km level distribution. It is characterized by ℓ^n = 1; r_o = 6.0 provides the best fit.

Figures 11 and 12 illustrate the 2.6σ-km level distribution. It is characterized by ℓ^n = 0.

Figures 13 and 14 illustrate the 2.9σ-km level distribution. It is probably an ℓ^n = 2 distribution; however, the fit is somewhat ambiguous at both values of r_o.

Figure 15 illustrates the 3.2σ-km level distribution. No determination of ℓ^n is possible. The asymmetry about 90 degrees suggests that sampling action takes place in the formation of this level, but it does not appear to be the characteristic "Gaussian" type.

Figures 16 and 17 illustrate the 3.5σ-km level distribution. It is probably an ℓ^n = 2 distribution; the fit is ambiguous with r_o = 6.0.

Figures 18 and 19 illustrate the 3.9σ-km level distribution. The data do not justify the assignment of ℓ^n. There is doubt whether the characteristic "Gaussian" type sampling takes place in the formation of this level. For comparison only, ℓ^n = 3 curves are shown.

Figures 20 and 21 illustrate the 3.8σ-km level distribution. It is probably an ℓ^n = 2 distribution, but the fit is poor. The assignment of ℓ^n might have been more definite had the level not been observed at 30 and 35 degrees.

Table IV tabulates the assignments of spin and parity to the states of Ca^{45} made as a result of the conclusions drawn above.

The intensity of the peaks from the various levels at their maxima was compared with the intensity of the ground state at $\theta = 40$ degrees, in order to calculate the relative differential cross sections. These relative cross sections and the angle at which they were compared are tabulated in Table IV. In these calculations, solid-angle corrections were used to correct for the different locations of the proton groups. The solid-angle corrections were taken from a curve prepared by S. F. Zimmerman, Jr, of this laboratory.

An attempt was made to determine absolute cross sections by comparison of the observed intensities of the (d,p) reactions with the intensity of Rutherford scattering of 5.0-Mev alpha-particles by Ca^{44}. This proved not to be possible with the gold-backed targets available, because the peak of the alpha-particles scattered by gold was wide enough to obscure the Ca^{44} peak.

The Butler curves, as calculated, represent only the angular distributions. A multiplying factor was required to apply to each calculated curve in order to match the maximum to the maximum of the experimental data. The factor for the 2.40-Mev level was obtained by matching the Butler curve to the experimental data at $\theta = 10$ degrees. The factors are listed in Table V. The factors are normalized so as to be equal to unity for the $\ell_n = 1$, $r_o = 6.0$, Butler curve. A solid-angle correction was made.

TABLE IV

Tabulation of Results

Peak	Q (Mev)	Excitation (Mev)	ℓ_n	Parity	Possible Values of Spin	Differential Cross Section Relative to Ground State at 40° ± 5 percent.	θ
0	5.19	0	3	Odd	5/2, 7/2	1.0	40°
1	5.01	0.18	-	-	-	≤0.05	all
2	3.76	1.43	1	Odd	1/2, 3/2	1.95	20°
3	3.30	1.89	1	Odd	1/2, 3/2	11.3	20°
4	2.94	2.25	1	Odd	1/2, 3/2	1.87	15°
5	2.79	2.40	0	Even	1/2	1.83	7-1/2°
6	2.35	2.84	1 or 2	-	1/2, 3/2, 5/2	2.06	20°
7	2.23	2.96	-	-	-	0.18	35°
8	1.95	3.24	1 or 2	-	1/2, 3/2, 5/2	0.991	20°
9	1.87	3.32	-	-	-	0.180	40°
10	1.77	3.42	1 or 2	-	1/2, 3/2, 5/2	4.17	15°

TABLE IA

Typical solution of Question

Item	x_i (mm)	Entries (mm)	π	Working	Entries to be applied to x_i	Estimated value of θ	θ
0	2·26	0	1	—	—	Difference between estimated value of θ and assumed value of θ $\pm$ 2 decimals	P_{00}
1	2·01	0·18	1	neg	$\pm 1.5, \pm 3.5, \pm 5$	1·0	T_{10}
2	3·32	0·25	1	neg	$\pm 1.5, \pm 3.5, \pm 5$	± 0.02	S_{01}
3	3·30	1·42	1	neg	$\pm 1.5, \pm 3.5, \pm 5$	1·42	S_{02}
4	3·98	0·52	1	neg	$\pm 1.5, \pm 3.5, \pm 5$	1·44	T_{20}
5	3·98	1·42	1	neg	$\pm 1.5, \pm 3.5, \pm 5$	1·43	S_{03}
6	3·32	0·25	1	neg	$\pm 1.5, \pm 3.5, \pm 5$	0·04	S_{11}
7	3·98	0·52	—	—	—	0·04	R_{20}
8	3·98	1·42	—	—	—	0·04	S_{12}
9	3·98	0·52	1	neg	$\pm 1.5, \pm 3.5, \pm 5$	0·04	T_{30}
10	3·98	1·42	1	neg	$\pm 1.5, \pm 3.5, \pm 5$	1·44	P_{00}

TABLE V

Ca^{45} Level	Butler Curve ℓ_n	r_o	Relative Multiplying Factor
Ground State	3	6.0	2.59
"	3	7.0	1.47
1.43-Mev Level	1	6.0	1.00
"	1	7.0	0.71
1.89-Mev Level	1	6.0	5.34
"	1	7.0	4.01
"	2	7.0	7.18
2.25-Mev Level	1	6.0	0.78
"	1	7.0	0.56
2.40-Mev Level	0	6.0	0.76
"	0	7.0	0.70
2.84-Mev Level	1	6.0	0.78
"	2	6.0	1.56
"	1	7.0	0.56
"	2	7.0	1.02
3.24-Mev Level	1	6.0	0.33
"	2	6.0	0.71
"	2	7.0	0.46
3.32-Mev Level	3	6.0	0.27
"	3	7.0	0.17
3.42-Mev Level	1	6.0	1.34
"	2	6.0	2.83
"	2	7.0	1.93

TABLE V

Cuts	Master Curve		Residuum Weighting Factor
	ℓ	π_e	
Ground Parts	3	6.0	2.79
"	3	7.0	1.47
1.45-Mev Level	1	6.0	1.00
"	1	7.0	0.71
1.90-Mev Level	1	6.0	5.45
"	1	7.0	4.03
"	2	7.0	1.18
2.35-Mev Level	1	6.0	0.78
"	1	7.0	0.56
2.60-Mev Level	0	6.0	0.76
"	0	7.0	0.70
2.75-Mev Level	1	6.0	0.78
"	2	6.0	1.56
"	1	7.0	0.46
"	2	7.0	1.08
3.05-Mev Level	1	6.0	0.33
"	2	6.0	0.71
"	2	7.0	0.46
3.20-Mev Level	3	6.0	0.27
"	3	7.0	0.17
3.42-Mev Level	1	6.0	1.38
"	2	6.0	2.73
"	2	7.0	1.93

IV. CONCLUSIONS

Agreement with the Butler theory seems adequate to assign values of ℓ_n with assurance to the distributions for the ground state and first five excited levels, with the exception of the first excited state. Assignment of ℓ_n to the distributions for the next five excited states is somewhat dubious.

It is emphasized that no unique value of r_o results in positive determinations of ℓ_n. It is further noted that those states assigned $\ell_n = 1$ were best fitted by $r_o = 6.0$, whereas the ground state, assigned $\ell_n = 3$, and the 2.84- and 3.24-Mev levels, with probable values of $\ell_n = 2$, are best fit by a higher r_o.

It is concluded that the Butler theory is not complete enough in all cases to make unambiguous assignments of ℓ_n. It appears that a more elaborate treatment is necessary.

Tobocman[20] has developed an extension of the Butler theory by considering the effect of Coulomb and nuclear interactions. The Coulomb effect would seem to be small, since the bombarding energy of 6.7 Mev in center-of-mass coordinates was above the Coulomb barrier of 5.6 Mev. However, only a slight shift of the maxima of the theoretical curves is required for good agreement with experiment.

According to Tobocman, the Coulomb interaction tends to move the maxima to larger angles and broaden the peaks and to fill the valleys between the primary and secondary maxima. However, the nuclear interaction tends to displace the peaks toward smaller angles

IV. CONCLUSIONS

Agreement with the Butler theory seems adequate to assign values of ℓ_n with assurance to the distributions for the ground state and first five excited levels, with the exception of the first excited state. Assignment of ℓ_n to the distributions for the next five excited states is somewhat dubious.

It is emphasized that no unique value of r_o results in positive determinations of ℓ_n. It is further noted that those states assigned $\ell_n = 1$ were best fitted by $r_o = 6.0$, whereas the ground states, assigned $\ell_n = 3$, and the 2.8$\frac{1}{2}$- and 3.2$\frac{1}{2}$-Mev levels, with probable values of $\ell_n = 2$, are best fit by a higher r_o.

It is concluded that the Butler theory is not complete enough in all cases to make unambiguous assignments of ℓ_n. It appears that a more elaborate treatment is necessary.

Tobocman[20] has developed an extension of the Butler theory by considering the effect of Coulomb and nuclear interactions. The Coulomb effect would seem to be small, since the bombarding energy of 6.7 Mev in center-of-mass coordinates was above the Coulomb barrier of 5.6 Mev. However, only a slight shift of the maxima of the theoretical curves is required for good agreement with experiment.

According to Tobocman, the Coulomb interaction tends to move the maxima to larger angles and broaden the peaks and to fill the valleys between the primary and secondary maxima. However, the nuclear interaction tends to displace the peaks toward smaller angles

and to make them less broad. A machine calculation is required to find the predicted position of the primary maxima according to the theory of Tobocman[21].

The data of this experiment make available for study the angular distributions of the ground state and six excited levels which appear to have almost pure stripping-type distributions. It is believed that the additional work necessary to make a machine calculation would be warranted in order to determine to what degree Tobocman's theory agrees with experiment.

and to make them less broad. A machine calculation is required to find the predicted position of the velocity maxima according to the theory of Tobocman[21].

The data of this experiment was available for study the angular distributions of the ground state and six excited levels which appear to have almost pure stripping-type distributions. It is believed that the additional work necessary to make a machine calculation would be warranted in order to determine to what degree Tobocman's theory agrees with experiment.

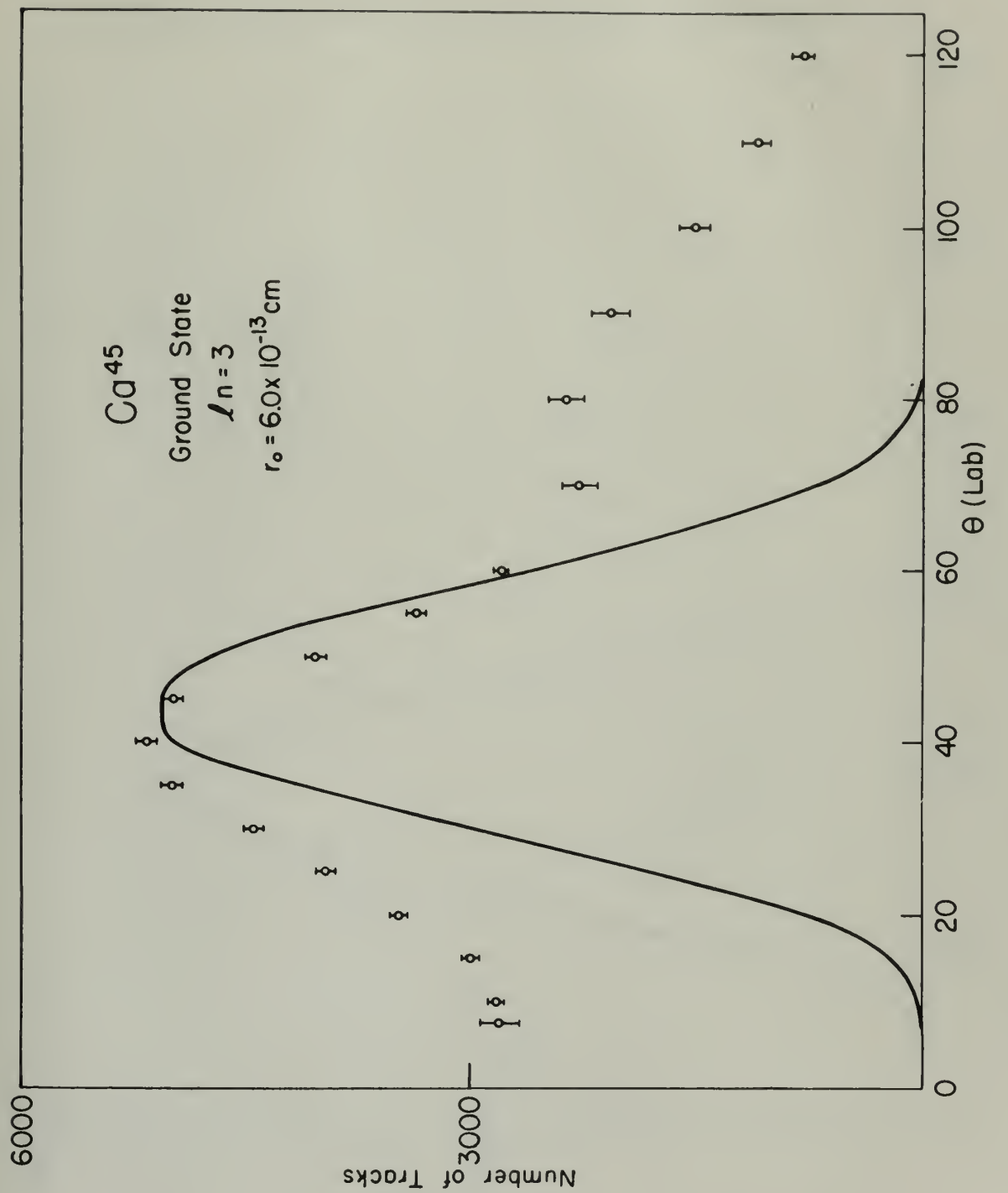
Ca45
Ground State
l n = 3
r₀ = 6.0x 10⁻¹³cm
Number of Tracks
6000
3000
0
20
40
60
80
100
120
θ (Lab)

Figure 3

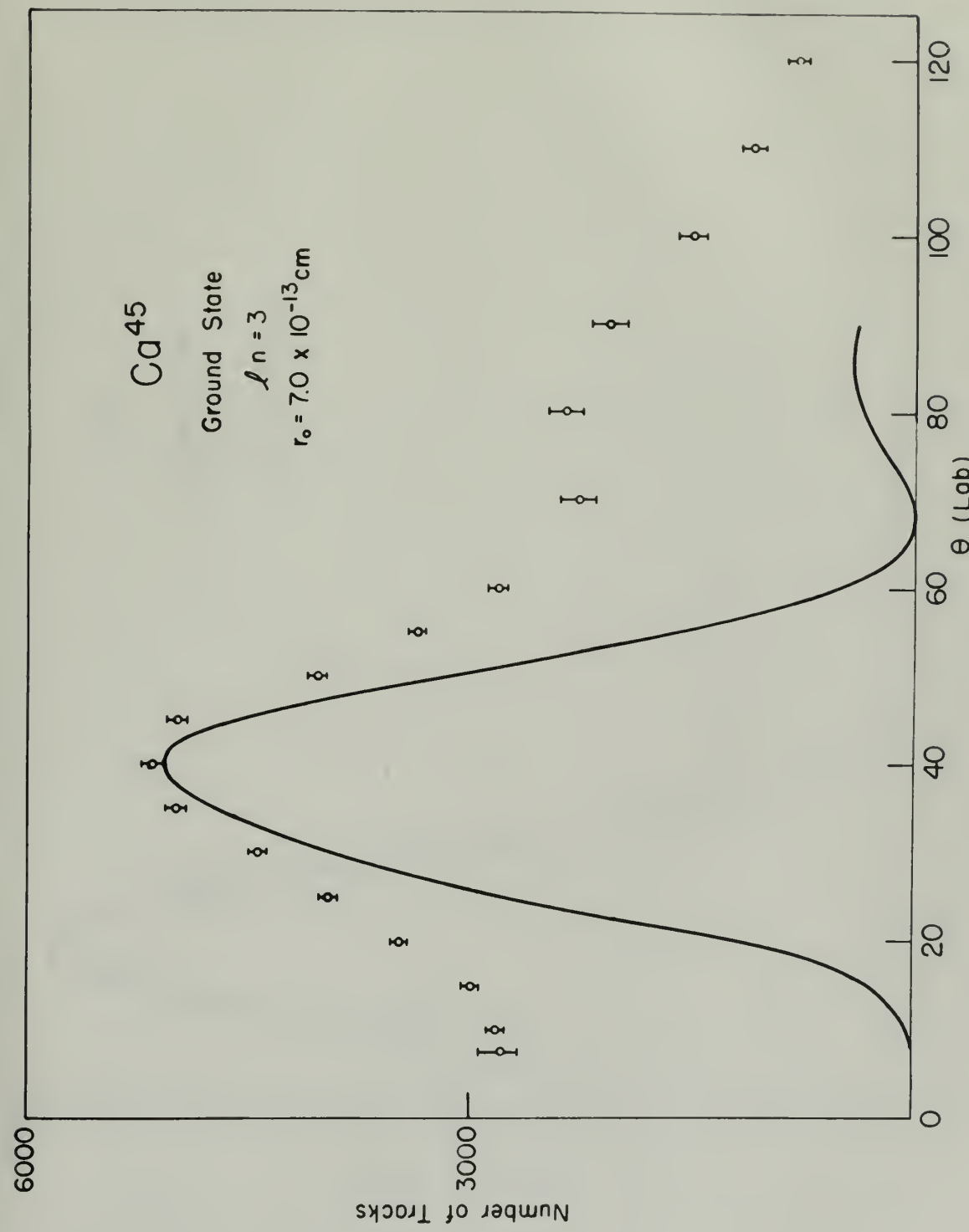
Ca45
Ground State
l n = 3
r₀ = 7.0 x 10⁻¹³cm
Number of Tracks
6000
3000
0
20
40
60
80
100
120
θ (Lab)

Figure 4

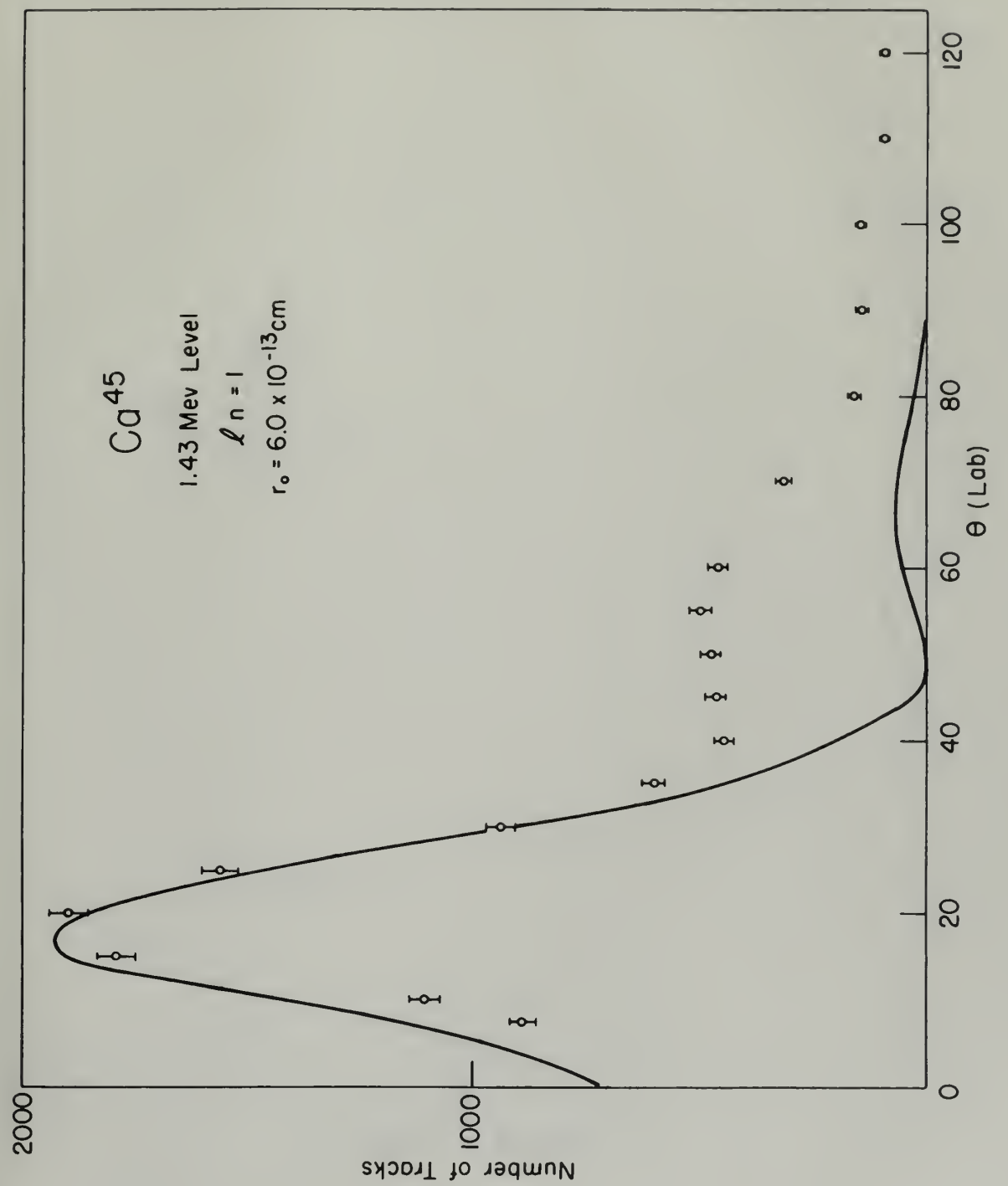
Ca45
1.43 Mev Level
ℓ n = 1
r₀ = 6.0 x 10⁻¹³cm
Number of Tracks
2000
1000
0
20
40
60
80
100
120
θ (Lab)

Figure 5

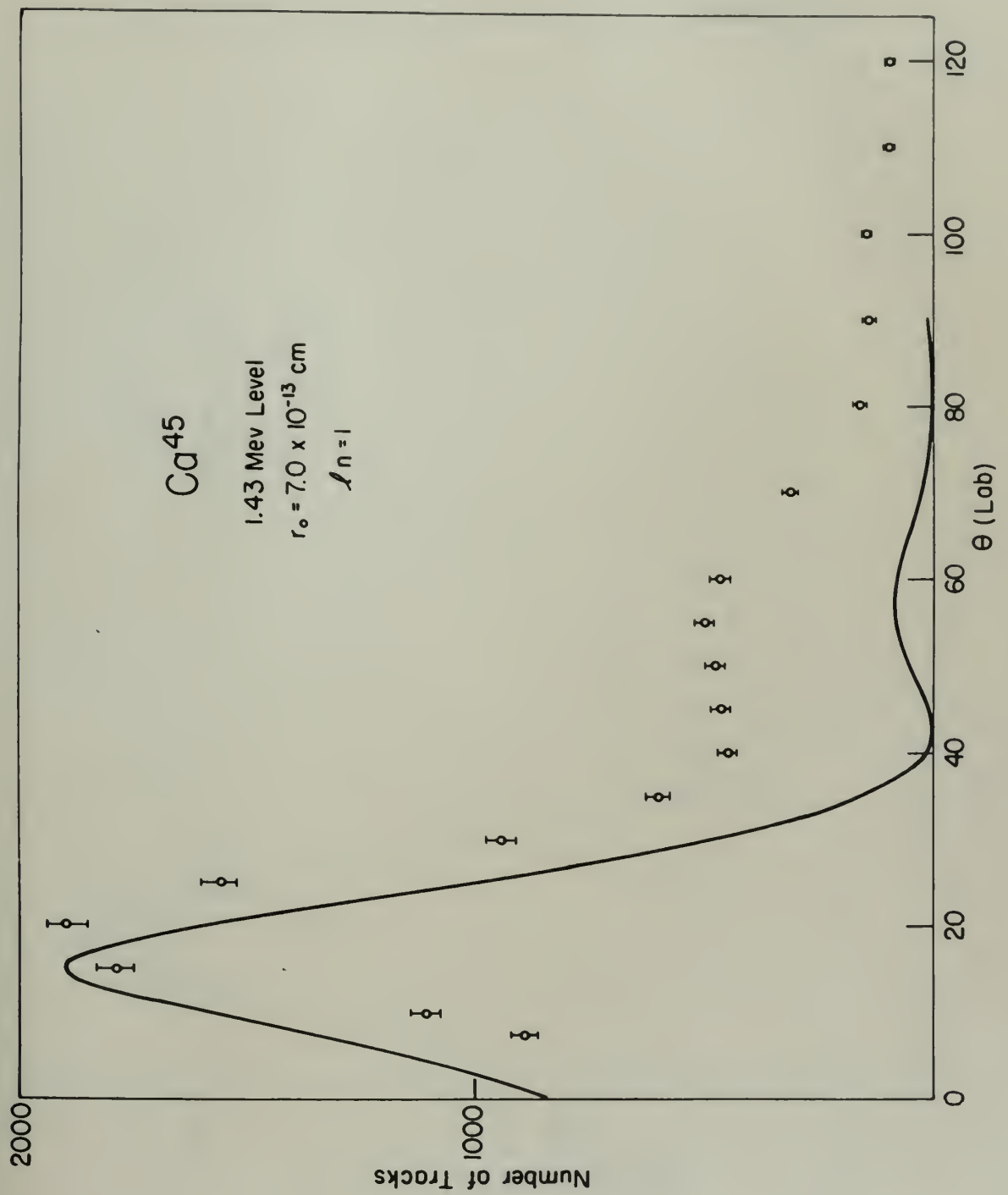
Ca45
1.43 Mev Level
$r_o = 7.0 \times 10^{-13}$ cm
$\ell n = 1$
Number of Tracks
2000
1000
0
20
40
60
80
100
120
θ (Lab)

Figure 6

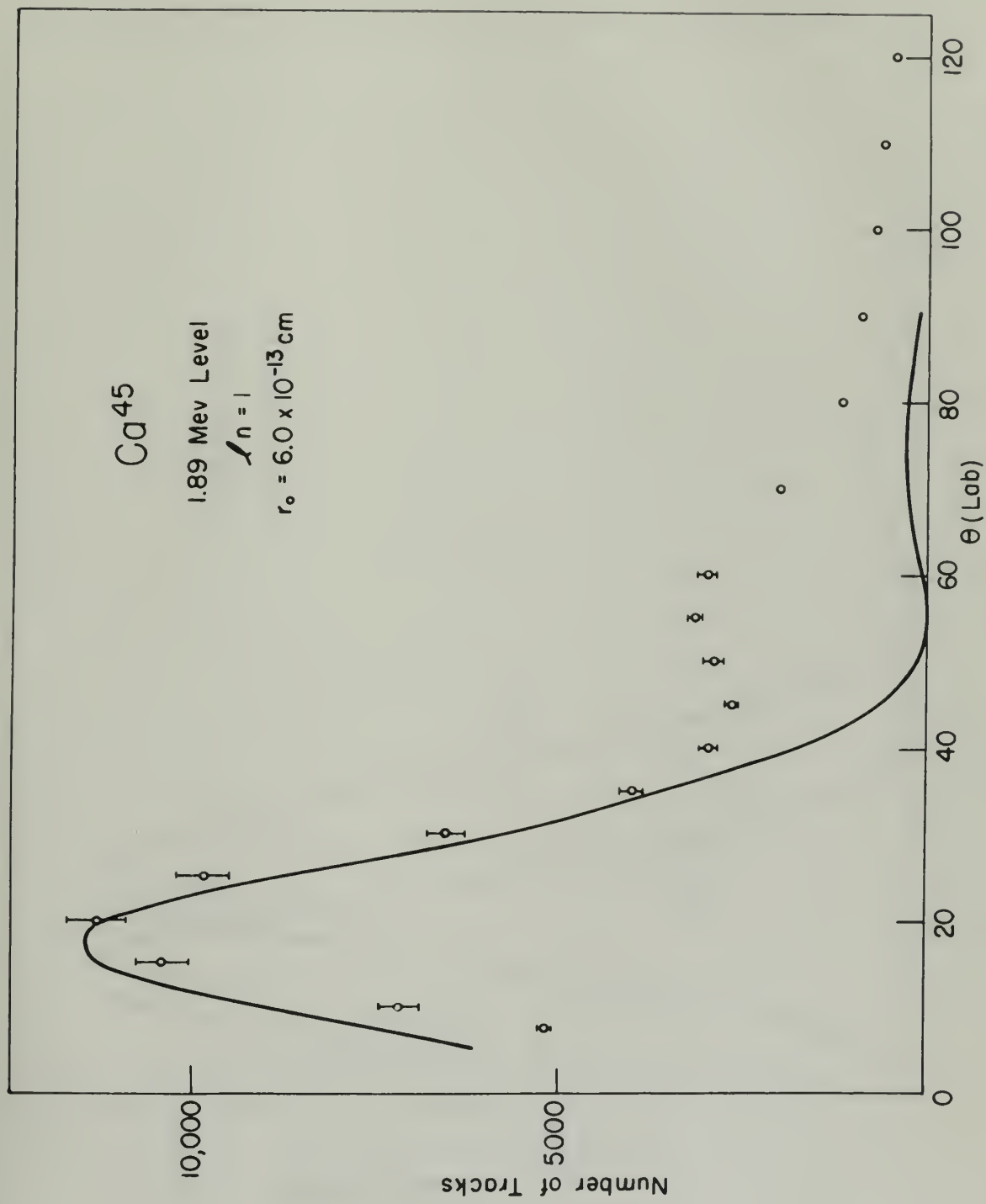
Ca45
1.89 Mev Level
l n = 1
r₀ = 6.0 x 10⁻¹³ cm
Number of Tracks
10,000
5000
0
20
40
60
80
100
120
θ (Lab)

Figure 7

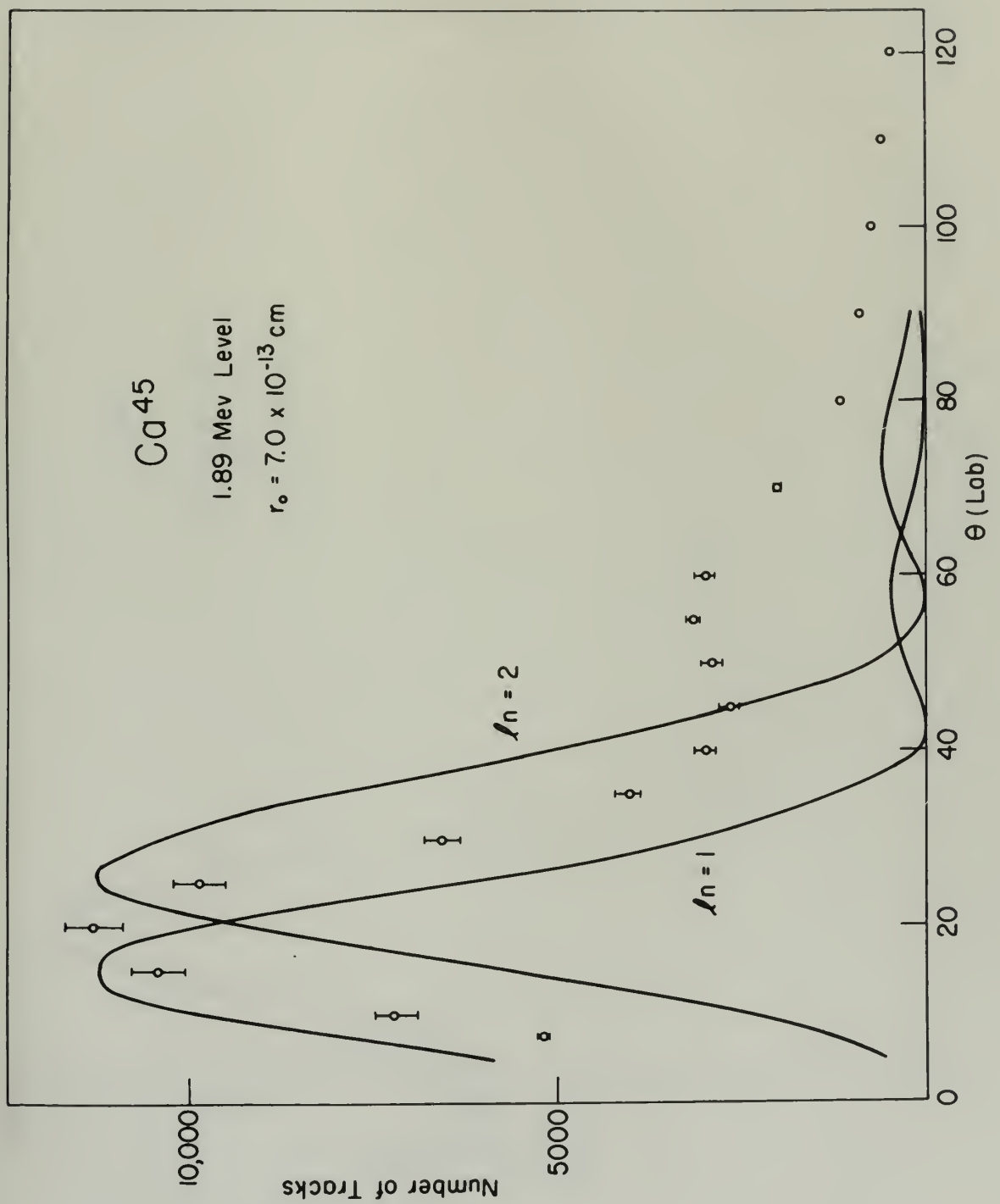
Ca45
1.89 Mev Level
$r_o = 7.0 \times 10^{-13}$ cm
$\ell_n = 2$
$\ell_n = 1$
Number of Tracks
10,000
5000
0
20
40
60
80
100
120
θ (Lab)

Figure 8

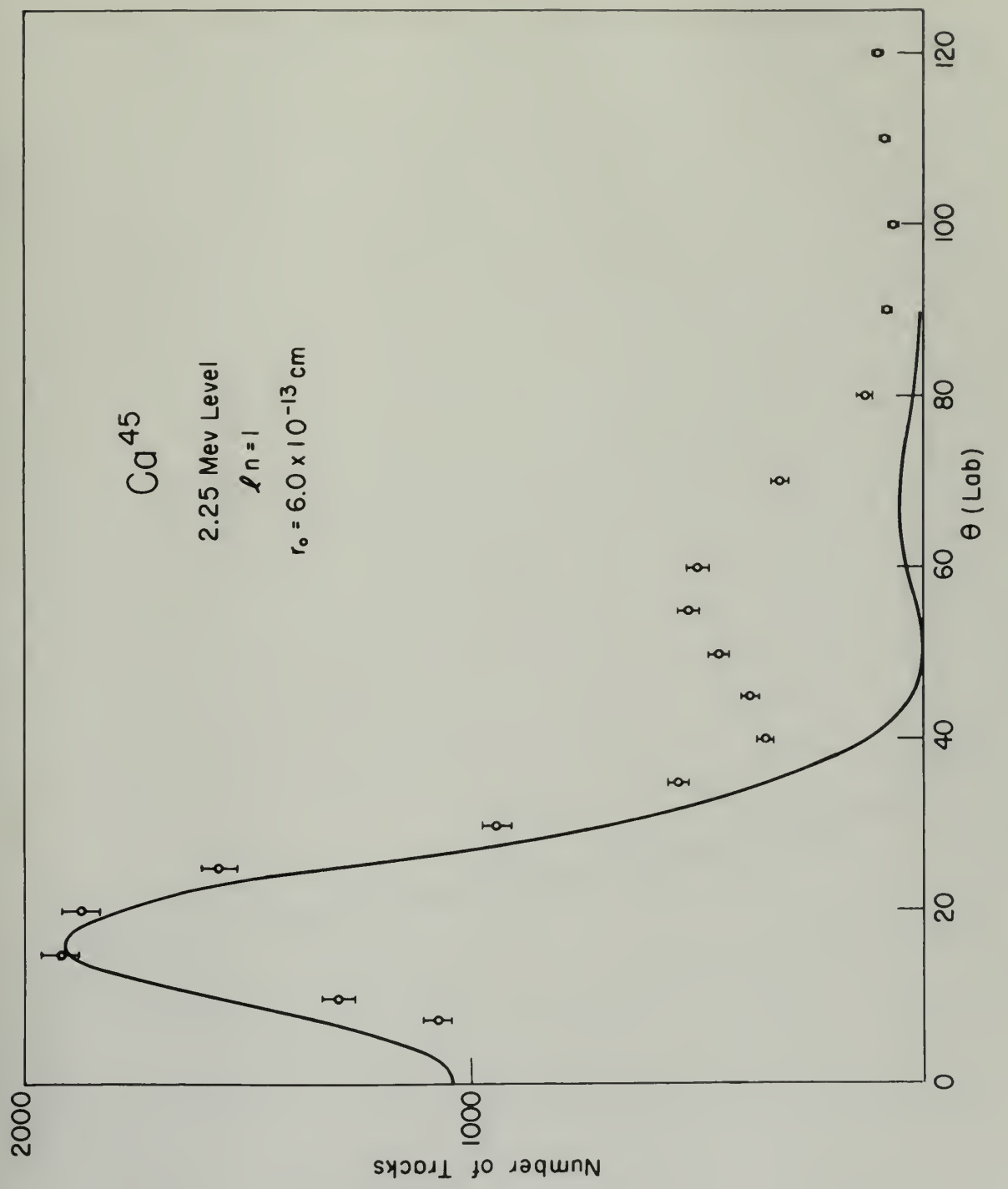
Ca45
2.25 Mev Level
ℓ n = 1
r₀ = 6.0 x 10⁻¹³ cm
Number of Tracks
2000
1000
0
20
40
60
80
100
120
θ (Lab)

Figure 9

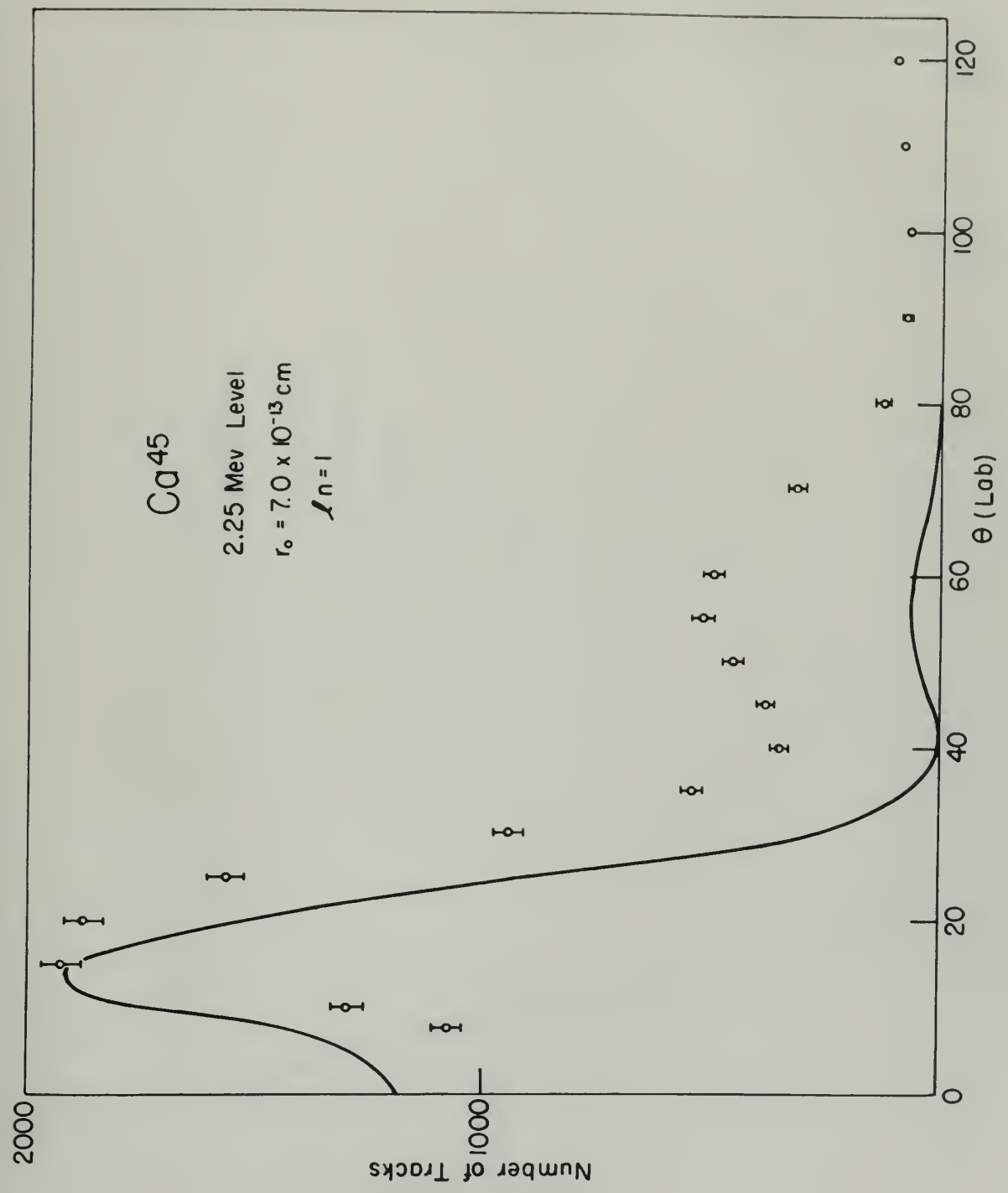
Ca45
2.25 Mev Level
$r_o = 7.0 \times 10^{-13}$ cm
$\ell n = 1$
Number of Tracks
2000
1000
0
20
40
60
80
100
120
θ (Lab)

Figure 10

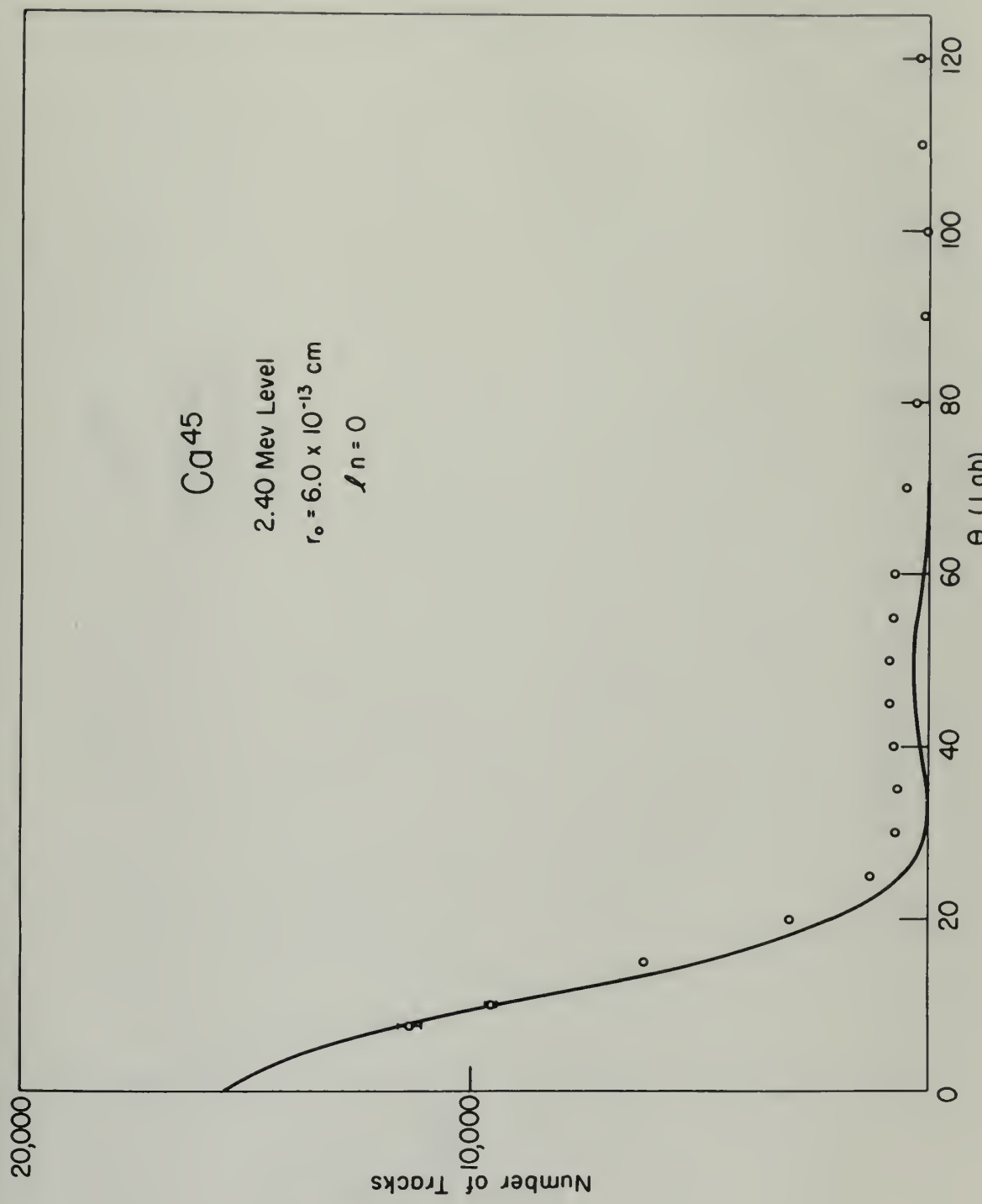
Ca 45
2.40 Mev Level
$r_o = 6.0 \times 10^{-13}$ cm
$\ell n = 0$
Number of Tracks
20,000
10,000
0
20
40
60
80
100
120
θ (Lab)

Figure 11

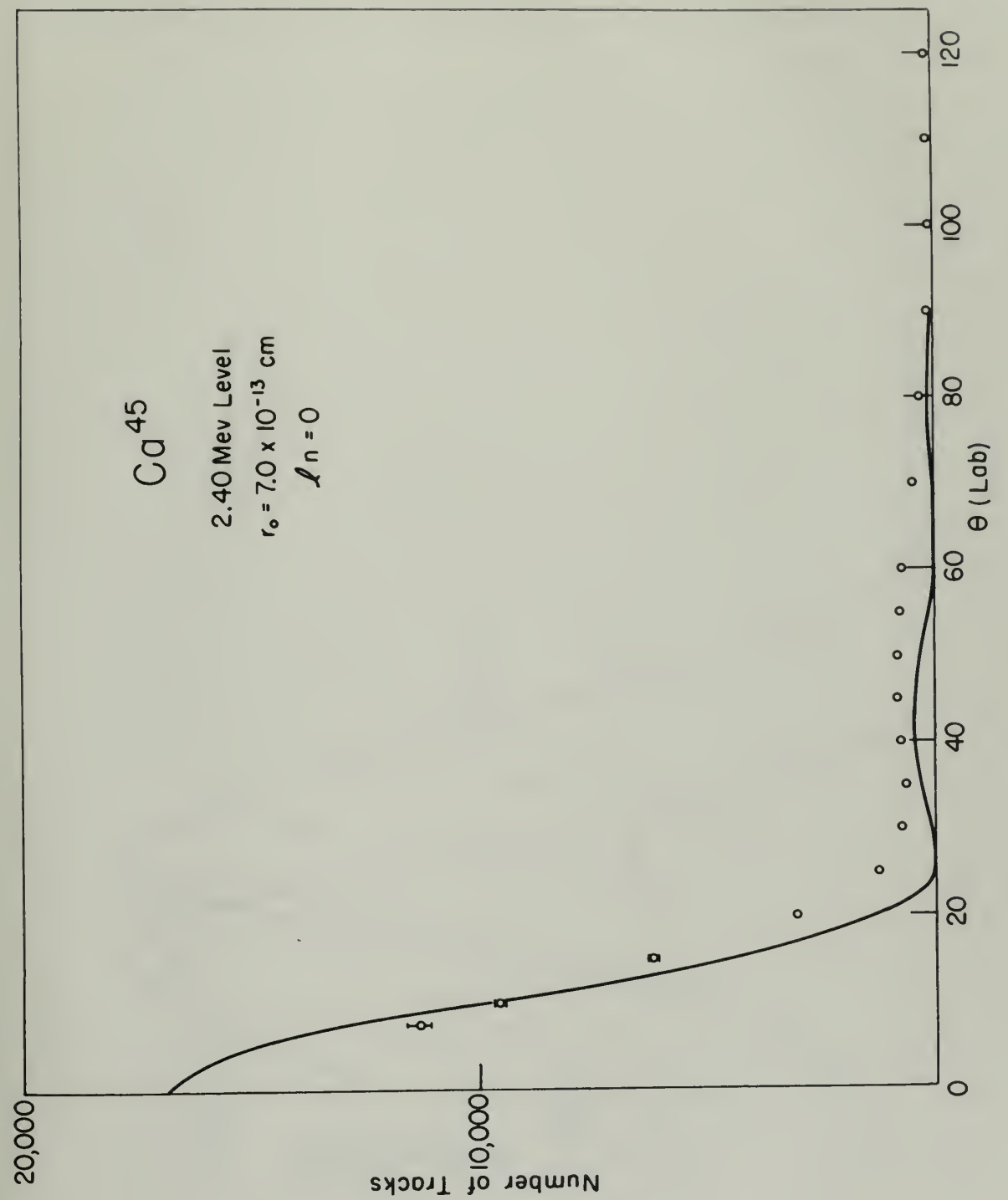
Ca45
2.40 Mev Level
r₀ = 7.0 x 10⁻¹³ cm
ℓn = 0
Number of Tracks
20,000
10,000
0
20
40
60
80
100
120
θ (Lab)

Figure 12

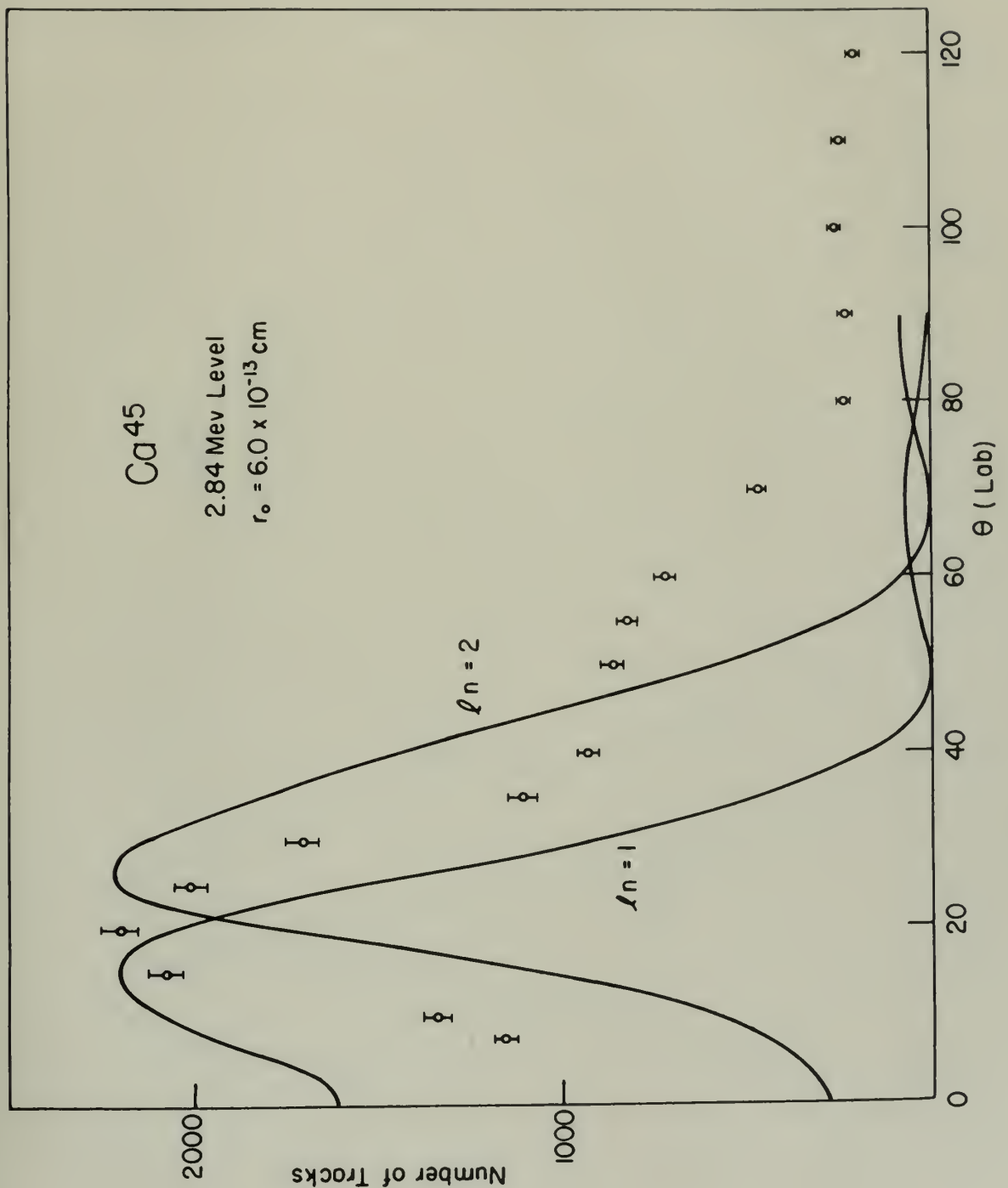
Ca 45
2.84 Mev Level
$r_o = 6.0 \times 10^{-13}$ cm
$\ell n = 2$
$\ell n = 1$
Number of Tracks
2000
1000
0
20
40
60
80
100
120
θ (Lab)

Figure 13

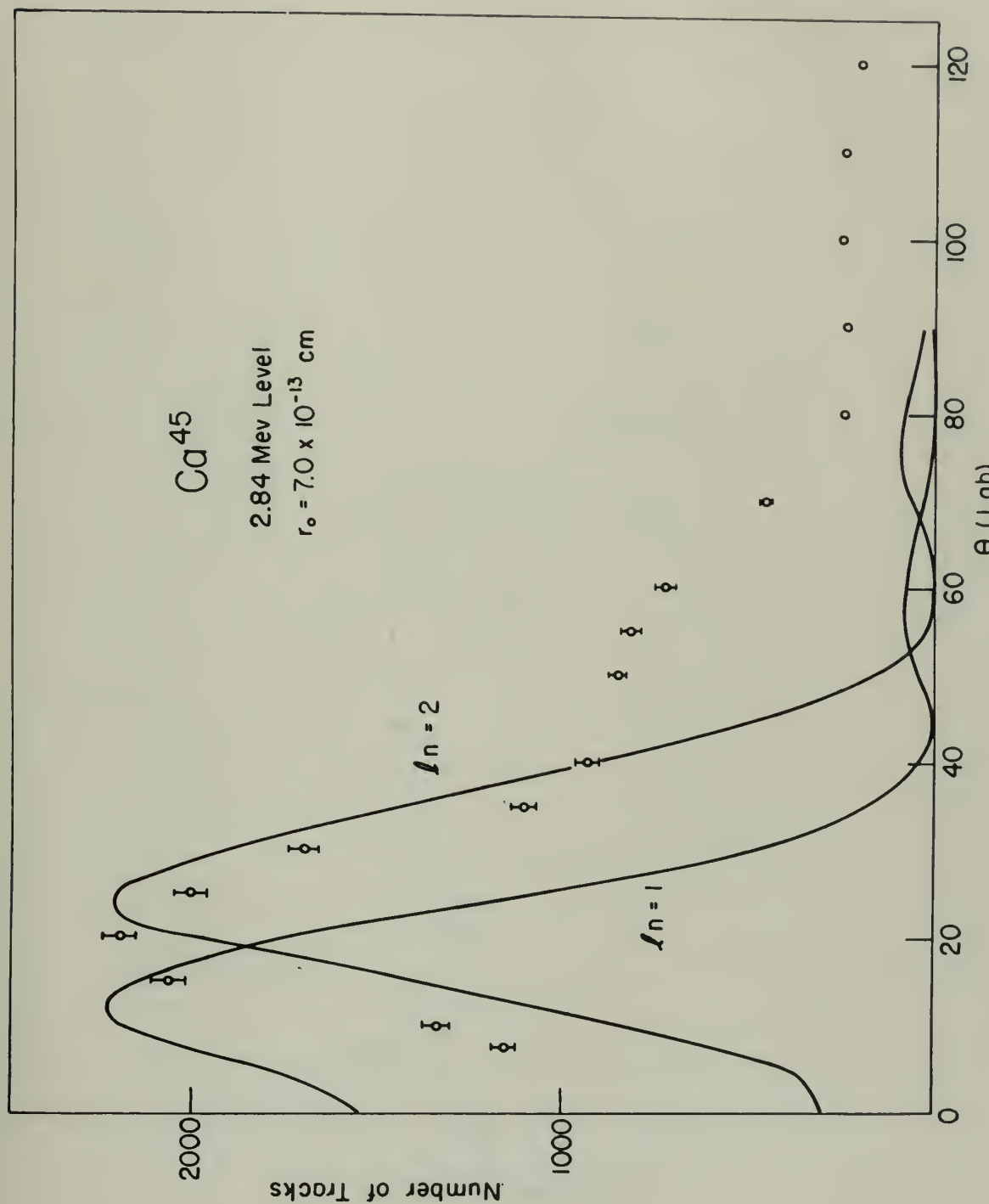
Ca45
2.84 Mev Level
r₀ = 7.0 x 10⁻¹³ cm
ℓn = 2
ℓn = 1
Number of Tracks
2000
1000
0
20
40
60
80
100
120
θ (Lab)

Figure 14

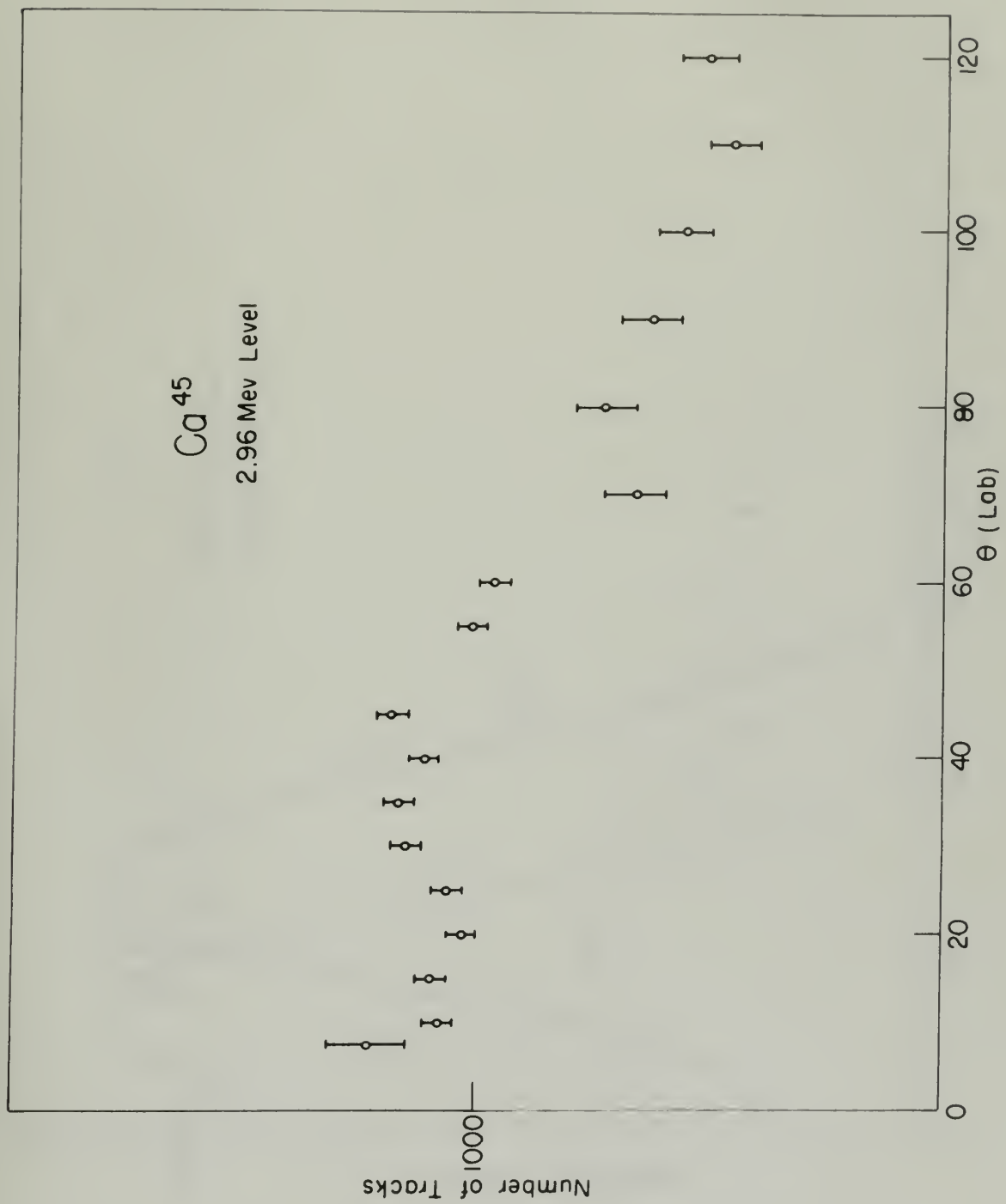
Ca 45
2.96 Mev Level
Number of Tracks
1000
0
20
40
60
80
100
120
θ (Lab)

Figure 15

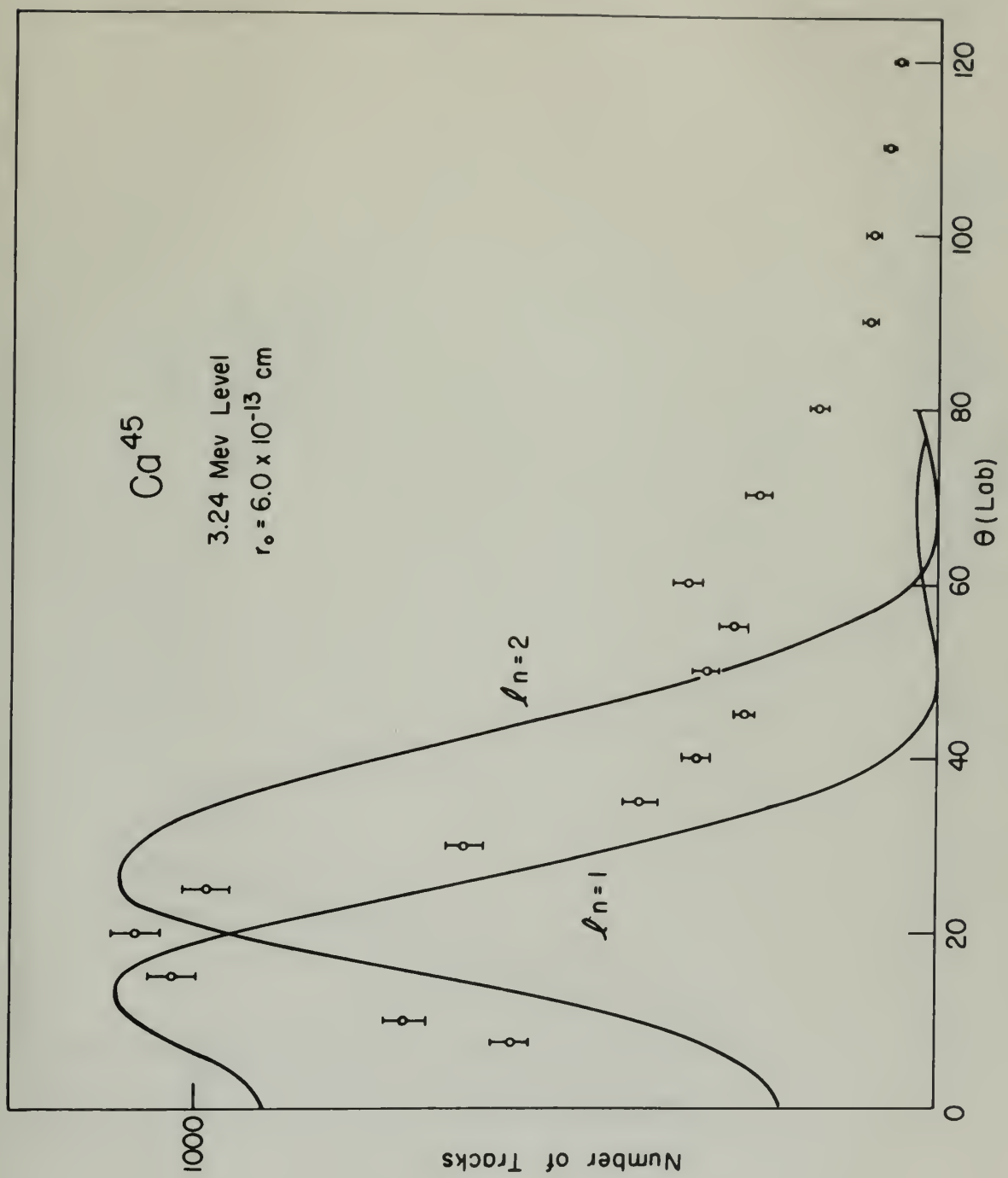
Ca45
3.24 Mev Level
r₀ = 6.0 x 10⁻¹³ cm
ℓn=2
ℓn=1
Number of Tracks
1000
0
20
40
60
80
100
120
θ(Lab)

Figure 16

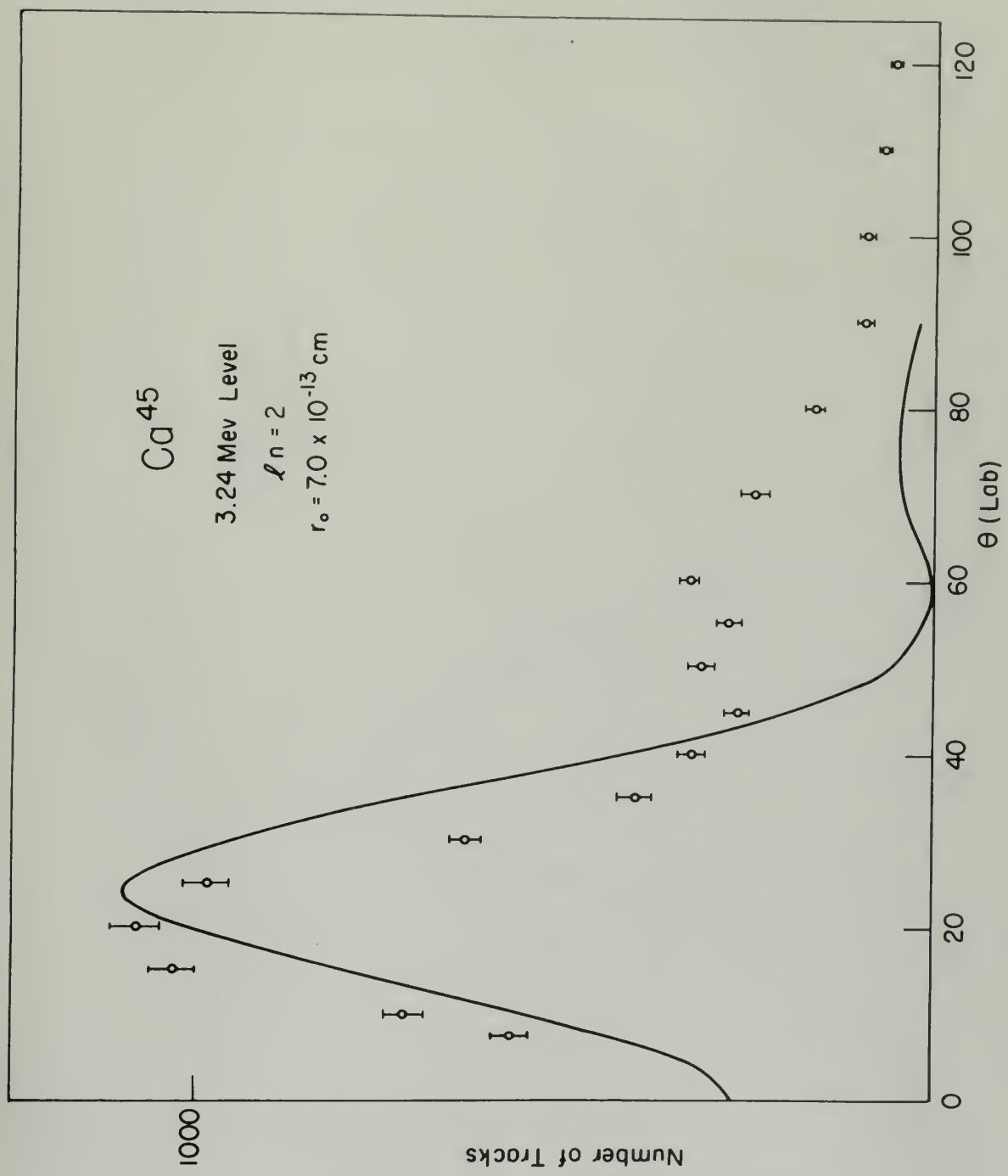
Ca45
3.24 Mev Level
ℓ n = 2
r₀ = 7.0 x 10⁻¹³ cm
Number of Tracks
1000
0
20
40
60
80
100
120
θ (Lab)

Figure 17

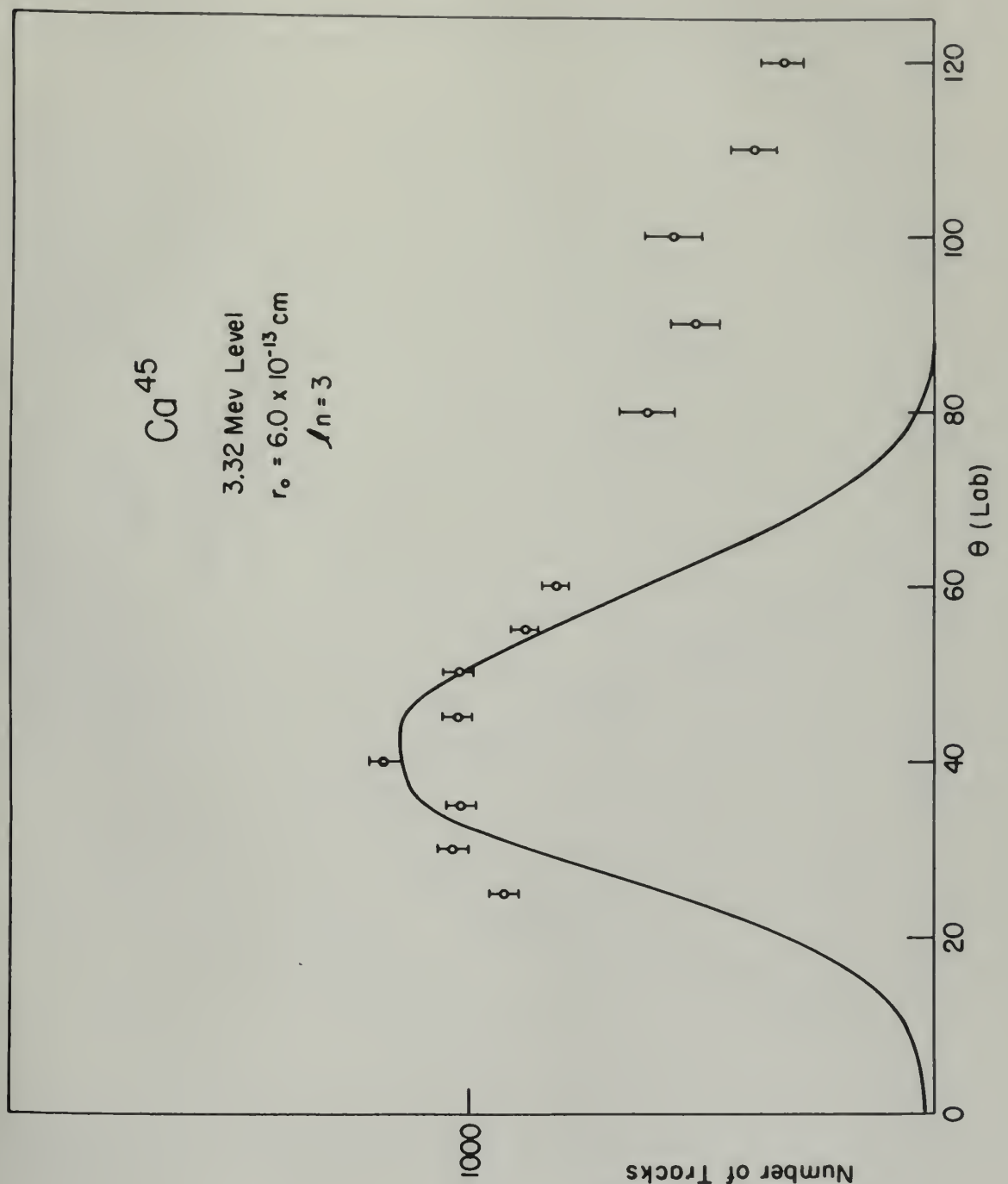
Ca45
3.32 Mev Level
r₀ = 6.0 x 10⁻¹³ cm
ℓn = 3
Number of Tracks
1000
0
20
40
60
80
100
120
θ (Lab)

Figure 18

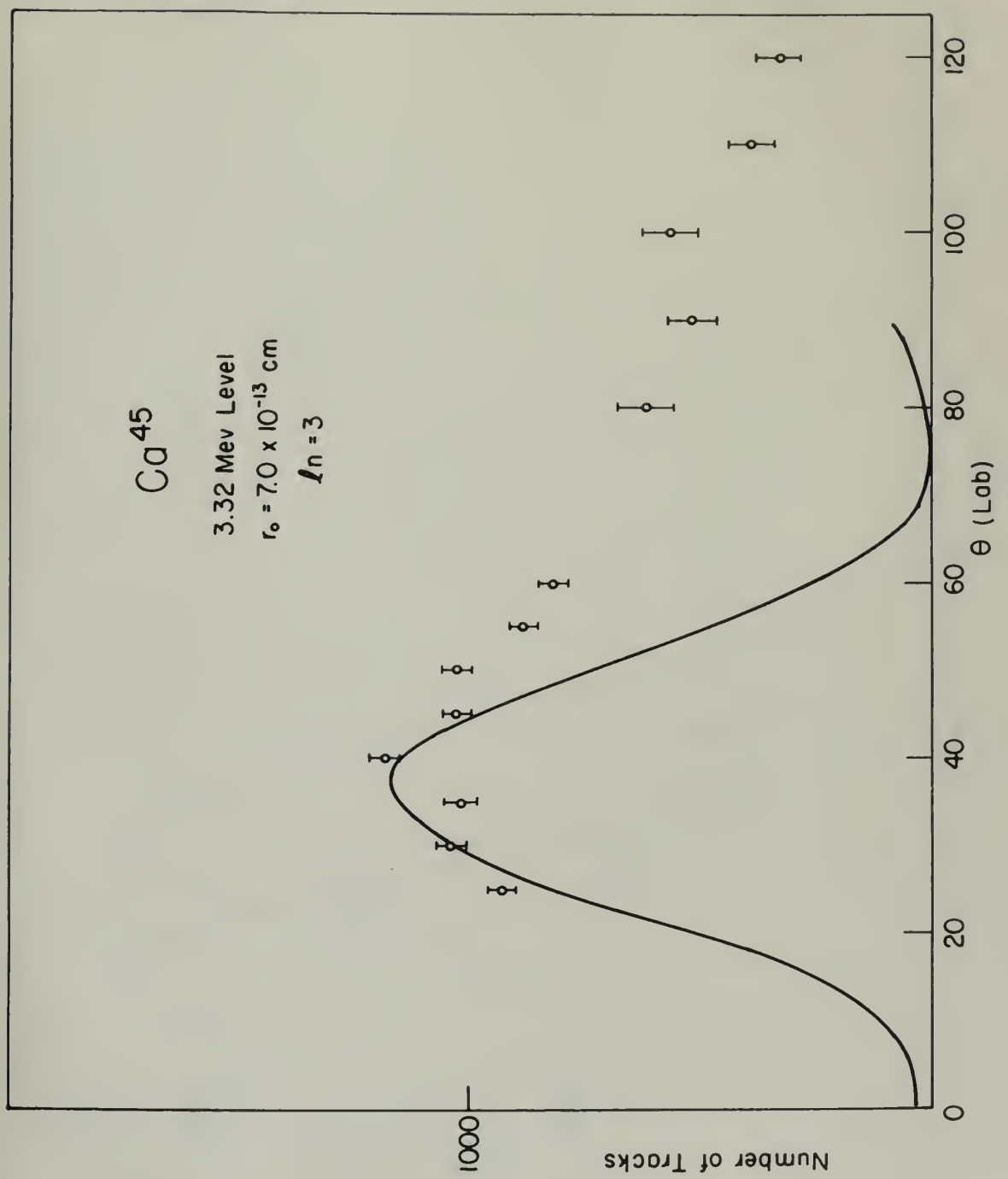
Ca45
3.32 Mev Level
r₀ = 7.0 x 10⁻¹³ cm
ℓn = 3
Number of Tracks
1000
0
20
40
60
80
100
120
θ (Lab)

Figure 19

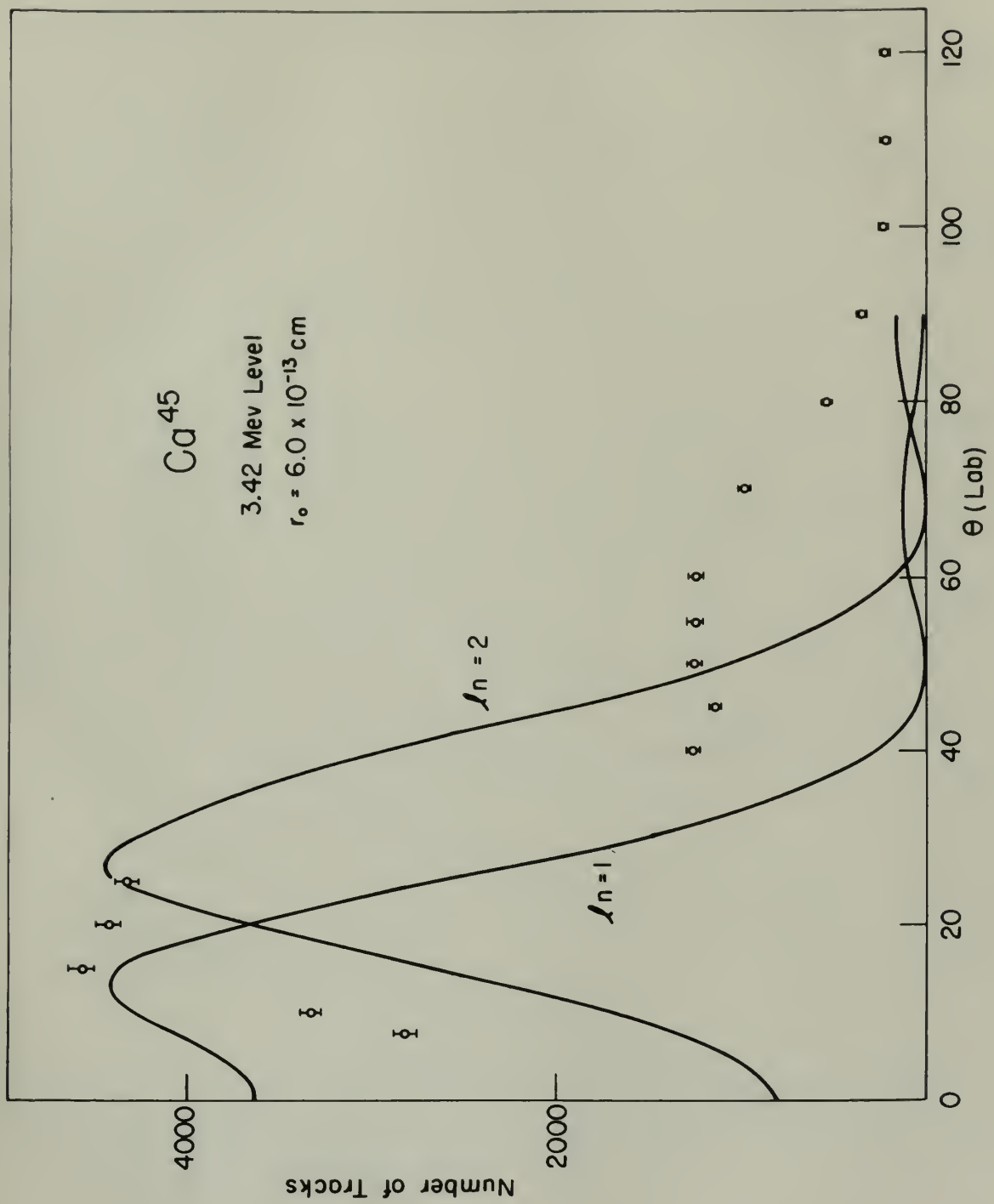
Ca45
3.42 Mev Level
r₀ = 6.0 x 10⁻¹³ cm
ℓn = 2
ℓn = 1
Number of Tracks
4000
2000
0
20
40
60
80
100
120
θ (Lab)

Figure 20

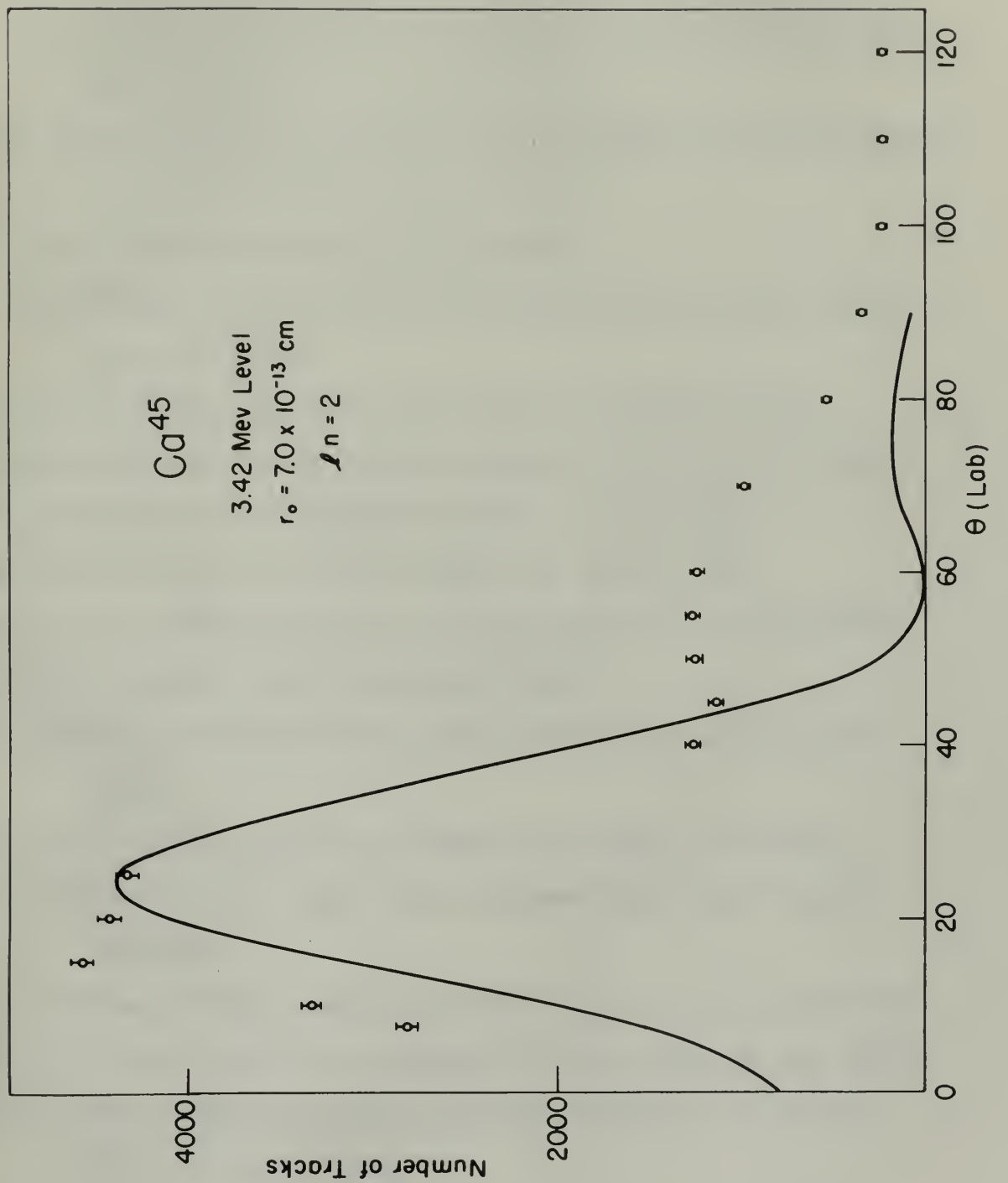
Ca45
3.42 Mev Level
r₀ = 7.0 x 10⁻¹³ cm
ℓ n = 2
Number of Tracks
4000
2000
0
20
40
60
80
100
120
θ (Lab)

Figure 21

REFERENCES

1. D. Kurath, Phys. Rev. 91, 1430 (1953).
2. A. R. Edmonds and B. H. Flowers, Proc. Roy. Soc. (London), A215, 120 (1952).
3. Braams, Bockelman, Browne, and Buechner, Phys. Rev. 474, 91 (1953).
4. C. M. Braams, Phys. Rev. 763, 94 (1954).
5. C. M. Braams, Phys. Rev. 95, 650 (1954).
6. Bockelman, Braams, Buechner, and Cuthe, Bull. Amer. Phys. Soc. 30, No. 3, 55 (1955).
7. S. T. Butler, Proc. Roy. Soc. (London), A208, 559 (1951).
8. C. M. Braams, Nuclear Science Abstracts, Vol. 8, No. 18B (1954).
9. H. Schuler and T. Schmidt, Naturwiss. 22, 758 (1934).
10. W. G. Proctor and F. C. Yu, Phys. Rev. 81, 20 (1951).
11. C. F. G. Delaney and H. H. J. Poole, Phys. Rev. 89, 529 (1953).
12. B. H. Ketelle, Phys. Rev. 80, 758 (1950).
13. Buechner, Sperduto, Browne, and Bockelman, Phys. Rev. 91, 1502 (1953).
14. G. M. Foglesong and D. G. Foxwell, M.S. Thesis, MIT (1954).
15. Buechner, Browne, Enge, Mazari, and Buntschuh, Phys. Rev. 95, 609 (1954).
16. Buechner, Strait, Sperduto, and Malm, Phys. Rev. 76, 1543 (1949).
17. C. R. Lubitz and W. C. Parkinson, Rev. Sci. Inst. 26, 400 (1955).
18. R. Huby, Progress in Nuclear Physics, edited by O. R. Frisch, Vol. 3, Sect. 7 (1953).

REFERENCES

1. D. Hurwitz, Phys. Rev. 91, 1430 (1953).

2. A. R. Edmonds and R. H. Pierens, Proc. Roy. Soc. (London), A221, 120 (1952).

3. Hansen, Nielsen, Bruene, and Bronsart, Phys. Rev. 117, 91 (1960).

4. C. M. Braams, Phys. Rev. 763, 91 (1954).

5. C. M. Braams, Phys. Rev. 95, 650 (1954).

6. Nielsen, Braams, Deutsch, and Curtis, Bull. Amer. Phys. Soc. 30, No. 3, 55 (1955).

7. S. T. Butler, Proc. Roy. Soc. (London), A208, 559 (1951).

8. C. M. Braams, Nuclear Science Abstracts, Vol. 8, No. 168 (1954).

9. H. Schuler and T. Schmidt, Naturwiss. 22, 758 (1934).

10. W. G. Proctor and F. C. Yu, Phys. Rev. 81, 20 (1951).

11. C. F. G. Delaney and H. H. Poole, Phys. Rev. 89, 529 (1953).

12. H. W. Retallack, Phys. Rev. 80, 758 (1950).

13. Hamilton, Spreduto, Brown, and Nielsen, Phys. Rev. 91, 1502 (1953).

14. G. M. Temmer and D. G. Pomerantz, U.S. Tests, NYU (1954).

15. Hamilton, Brenne, Ingo, Ebert, and Buntschuh, Phys. Rev. 95, 609 (1954).

16. Hamilton, Ebert, Sperduto, and Ibin, Phys. Rev. 76, 1413 (1949).

17. G. R. Lichte and W. C. Parkinson, Rev. Sci. Inst. 26, 400 (1955).

18. R. Hofp, Progress in Nuclear Physics, edited by O. R. Frisch, Vol. 3, Sect. 7 (1953).

19. G. Gamow and C. L. Critchfield, Theory of Atomic Nucleus and Nuclear Energy Sources, Clarendon Press, Oxford (1950).

20. W. Tobocman, Phys. Rev. 94, 1655 (1954).

21. W. Tobocman and M. H. Kalos, Phys. Rev. 97, 132 (1955).

19. G. Gamow and C. L. Critchfield, Theory of Atomic Nucleus and Nuclear Energy Sources, Clarendon Press, Oxford (1950).

20. W. Tobocman, Phys. Rev. 91, 1657 (1953).

21. W. Tobocman and M. H. Kalos, Phys. Rev. 97, 132 (1955).